

# Multi-entropy from Linking in Chern-Simons Theory

---

**Ma-Ke Yuan,<sup>a</sup> Mingyi Li<sup>a</sup> and Yang Zhou<sup>a,b</sup>**

<sup>a</sup>*Department of Physics and Center for Field Theory and Particle Physics,  
Fudan University, Shanghai 200433, China*

<sup>b</sup>*Peng Huanwu Center for Fundamental Theory, Hefei, Anhui 230026, China*  
E-mail: [mkyuan19@fudan.edu.cn](mailto:mkyuan19@fudan.edu.cn), [limy22@m.fudan.edu.cn](mailto:limy22@m.fudan.edu.cn),  
[yang\\_zhou@fudan.edu.cn](mailto:yang_zhou@fudan.edu.cn)

**ABSTRACT:** We study the multipartite entanglement structure of quantum states prepared by the Euclidean path integral over three-manifolds with multiple torus boundaries (the so-called link states) in both Abelian and non-Abelian Chern-Simons theories. For three-component link states in the Abelian theory, we derive an explicit formula for the Rényi multi-entropy in terms of linking numbers. We further show that the genuine multi-entropy faithfully quantifies the tripartite entanglement generated by GHZ-states, consistent with the fact that the prepared states are stabilizer states.

---

## Contents

<b>1</b>	<b>Introduction</b>	<b>2</b>
<b>2</b>	<b>Review of (genuine) multi-entropy</b>	<b>3</b>
2.1	Multi-entropy	3
2.2	Genuine Rényi tri-entropy	5
2.3	Genuine Rényi quadri-entropy	7
<b>3</b>	<b>Genuine multi-entropy for torus link states</b>	<b>8</b>
3.1	Multi-boundary states in Chern-Simons theory	8
3.2	Abelian case	9
3.2.1	Three-component links	9
3.2.2	$N$ -component links	12
3.2.3	Quadri-entropy of four-component links	13
3.3	Non-Abelian case	13
3.3.1	Connected sum of two Hopf links	14
3.3.2	Link $\mathbf{6}_3^3$	16
3.3.3	Borromean rings	16
<b>4</b>	<b>Logarithmic negativity for three-component links</b>	<b>17</b>
4.1	Third-order negativity for three-links	19
<b>5</b>	<b>Entanglement structure of links</b>	<b>19</b>
5.1	Prime-power qudit stabilizer states	19
5.2	General qudit stabilizer states	21
5.3	Possible lower and upper bounds of the genuine tri-entropy	22
<b>6</b>	<b>Conclusion and discussion</b>	<b>23</b>
<b>A</b>	<b>Second genuine Rényi tri-entropy of generalized GHZ-states (2.14)</b>	<b>23</b>
<b>B</b>	<b>Derivation of (3.19)</b>	<b>24</b>
<b>C</b>	<b>Derivation of (4.8)</b>	<b>25</b>
<b>D</b>	<b>Non-rigorous proof of (4.13)</b>	<b>26</b>
<b>E</b>	<b>The Venn diagram</b>	<b>27</b>
<b>F</b>	<b>Genuine tri-entropy in (1+1)d Chern-Simons theory</b>	<b>28</b>

## 1 Introduction

Understanding multipartite entanglement has become increasingly important in both quantum field theory and holography. Within the framework of the AdS/CFT correspondence, multipartite entanglement among boundary degrees of freedom is believed to underlie the emergence of bulk spacetime geometry. From the field-theoretic perspective, multipartite entanglement serves as a refined probe of nonlocal quantum correlations, topological order, and critical phenomena, extending beyond the information captured by bipartite entanglement entropy. Developing quantitative and conceptual tools to characterize multipartite entanglement is therefore crucial for elucidating the microscopic organization of quantum many-body systems and for advancing our understanding of holographic duality.

In Ref. [1], the multi-entropy was introduced as a natural multipartite generalization of the entanglement entropy. Its definition is based on the replica trick (see Section 2.1 for a brief review), where one computes Rényi-type quantities for integer replica number and performs an analytic continuation to  $n = 1$ . In general, this continuation is technically challenging and often inaccessible in quantum field theory. In this work, we demonstrate that for link states in Chern-Simons theory, the analytic continuation can be carried out explicitly, leading to a closed-form expression for the tripartite multi-entropy of the three-component link state (3.23).

Another central result of this work is the discovery of a network of relations among different bipartite and tripartite entanglement measures for link states. These include the entanglement entropy, mutual information, logarithmic negativity (and the third-order negativity), as well as the genuine multi-entropy. Through these relations, we uncover the precise physical interpretation of the tripartite genuine multi-entropy and clarify its role in characterizing multipartite correlations beyond pairwise entanglement. In particular we show that the genuine multi-entropy faithfully quantifies the tripartite entanglement generated by GHZ-states, consistent with the fact that the prepared states are stabilizer states.

Our results also fit naturally into a broader line of recent developments on multipartite entanglement and the Rényi multi-entropy. For instance, studies of multipartite correlation measures include Refs. [2–4]; Refs. [5, 6] discuss bulk replica symmetry breaking in the context of Rényi multi-entropy; Ref. [7] provides a classification of multipartite entanglement; Refs. [8, 9] explore its monotonicity properties; Ref. [10] performs field-theoretical computations in two-dimensional CFTs at small Rényi index; Refs. [11, 12] study applications in topologically ordered systems; Ref. [13] extends the construction to mixed states and Ref. [14] further discusses the multipartite markov gaps; Refs. [15–17] formulate the genuine version of multi-entropy and also investigate applications to black hole information problems; and Ref. [18] employs Rényi multi-entropy to probe quantum critical points.

A particularly relevant line of research concerns link states in three-dimensional Chern-Simons theory, which provide concrete and topologically nontrivial realizations of multipartite entanglement. Entanglement entropy of link states has been analyzed in Refs. [19–22], while the relation between linking and quantum anomalies was explored in Refs. [23, 24]. Multipartite entanglement of link states was further investigated in Refs. [25, 26].

The remainder of this paper is organized as follows. In Section 2, we review the definitions and basic properties of the multi-entropy and the genuine multi-entropy. Section 3 is devoted to the study of genuine multi-entropy for link states in three-dimensional Chern-Simons theory, both in the Abelian and non-Abelian cases. In Section 4, we compute the entanglement negativity for three-component links. In Section 5, we clarify the physical meanings of genuine multi-entropy and logarithmic negativity for stabilizer states. Additional proofs and technical details are collected in the appendices.

**Note added:** While this paper was being completed, Ref. [27] appeared on the arXiv, which has some overlap with our multi-entropy results. We have added Appendix G to clarify the relation.

## 2 Review of (genuine) multi-entropy

### 2.1 Multi-entropy

Before introducing the multi-entropy, let us briefly review the concepts of entanglement entropy (EE) and Rényi entropy. Given a pure state  $|\psi\rangle$  and dividing the entire system into  $A$  and its complementary  $\bar{A}$ , the EE between them is defined as

$$S(A) = -\text{Tr}\rho_A \log \rho_A , \quad (2.1)$$

where  $\rho_A = \text{Tr}_{\bar{A}} |\psi\rangle \langle \psi|$  is the reduced density matrix. Rényi entropy is a one-parameter generalization of EE

$$S_n(A) = \frac{1}{1-n} \log \text{Tr}\rho_A^n , \quad (2.2)$$

and it reduces to EE (2.1) in the limit  $n \rightarrow 1$ . This method of computing EE is known as the *replica trick*. The Rényi entropy satisfies<sup>1</sup>

$$S_n(A) = S_n(\bar{A}) = S_n(A; \bar{A}) . \quad (2.3)$$

The  $\text{Tr}\rho_A^n$  part in the definition of Rényi entropy (2.2) can be reformulated through the permutation and contraction of the indices of the  $n$  copies of  $\rho_A$ ,

$$\begin{aligned} \rho_A^n &= (\rho_A)_{\alpha_1}^{\alpha_2} (\rho_A)_{\alpha_2}^{\alpha_3} (\rho_A)_{\alpha_3}^{\alpha_4} \cdots (\rho_A)_{\alpha_n}^{\alpha_1} \\ &= (\rho_A)_{\alpha_1}^{\alpha_{\sigma \cdot 1}} (\rho_A)_{\alpha_2}^{\alpha_{\sigma \cdot 2}} (\rho_A)_{\alpha_3}^{\alpha_{\sigma \cdot 3}} \cdots (\rho_A)_{\alpha_n}^{\alpha_{\sigma \cdot n}} . \end{aligned} \quad (2.4)$$

with  $\sigma = (123 \cdots n)$  the permutation acting on the index of replicas. Guided by this key observation, in [1] the authors defined the *multi-entropy*  $S^{(q)}$ , which generalizes the concept

---

<sup>1</sup>In this paper we sometimes use the notation  $S_n(A; \bar{A})$  to emphasize that it is the entanglement between  $A$  and its complement  $\bar{A}$ .

of EE to  $q$ -partite cases through the permutation and contraction of indices. Let us focus on tripartite pure state  $|\psi\rangle_{ABC}$  to illustrate.

Like Rényi entropy, after preparing several copies for the tripartite system, the entanglement measure  $S_n^{(q=3)}$  should be determined by the choice of permutation  $(\sigma_A, \sigma_B, \sigma_C)$  acting on the indices of different replicas, i.e., the way of contracting multiple density matrices. Note that there is an equivalence relation

$$(\sigma_A, \sigma_B, \sigma_C) \sim (\sigma_A, \sigma_B, \sigma_C) \cdot g \quad (2.5)$$

allowing us to consider only  $(q-1)$ -parties, i.e., we can always choose  $g = \sigma_A^{-1}$  to make  $\sigma_A = \text{id}$  and the entanglement measure is only determined by  $(\sigma_B, \sigma_C)$ .<sup>2</sup> Both  $B$  and  $C$  have  $n$  replicas and  $(\sigma_B, \sigma_C)$  are chosen to be cyclic permutations of order  $n$ . In total, we have  $n^{q-1} = n^2$  replicas, which form a  $n \times n$  square lattice. The multi-entropy is defined by choosing the replica symmetry as  $\mathbb{Z}_n \otimes \mathbb{Z}_n$  with the first/second  $\mathbb{Z}_n$  acting on the subregion  $B/C$  and cyclically permuting the replicas located in the same row/column of the lattice.

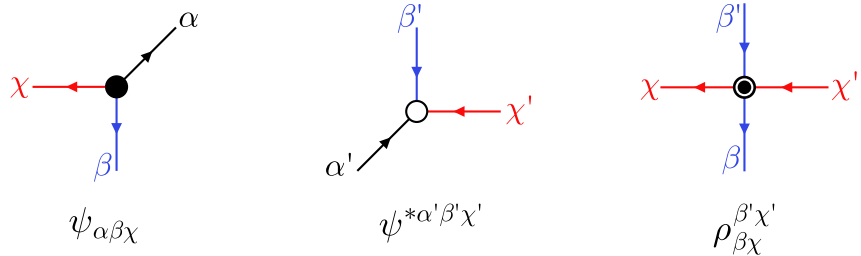


**Figure 1:** Graphical notation for the tripartite wavefunction  $\psi$ , its conjugate  $\psi^*$  and the reduced density matrix  $\rho_{BC}$ .

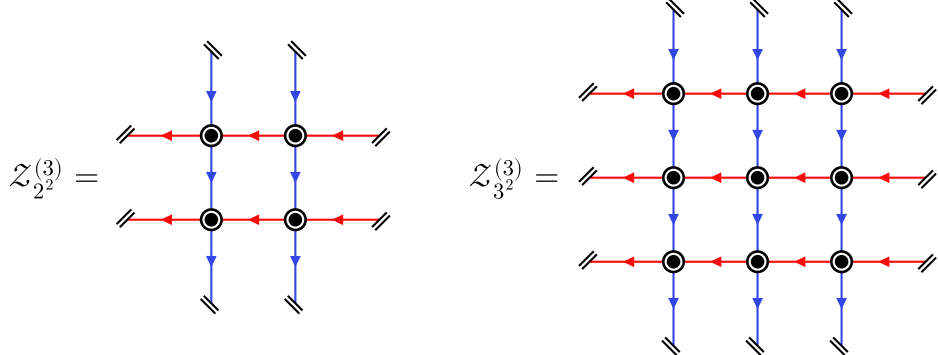


**Figure 2:** The construction of  $\mathcal{Z}_{n^{q-1}}^{(q)}$  in the special case  $q=3$  and  $n=2,3$ .

For general  $q$ -partite entanglement, the  $n$ -th Rényi multi-entropy is defined as<sup>3</sup>

$$S_n^{(q)} = \frac{1}{1-n} \frac{1}{n^{q-2}} \log \left( \mathcal{Z}_{n^{q-1}}^{(q)} / (\mathcal{Z}_1^{(q)})^{n^{q-1}} \right), \quad (2.6)$$

<sup>2</sup>In this paper, we treat all the subsystems symmetrically.

<sup>3</sup>Compared with [1], we use a slightly different notation here. We denote the partition function on the  $n^{q-1}$ -sheet Riemann surface by  $\mathcal{Z}_{n^{q-1}}^{(q)}$  instead of  $\mathcal{Z}_n^{(q)}$  in [1].

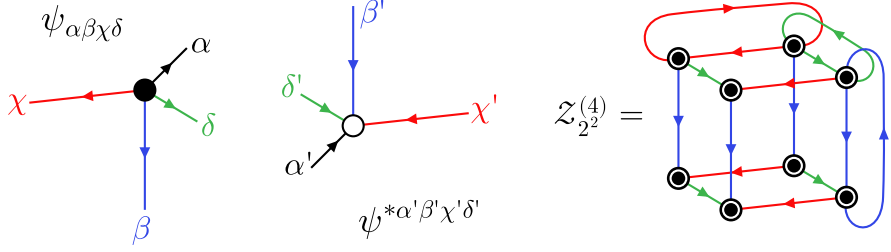


**Figure 3:** Graphical notation for the quadripartite wavefunction  $\psi$ , its conjugate  $\psi^*$ , and the construction of  $\mathcal{Z}_{2^4-1}^{(q=4)}$ . Note that for clarity we omitted some identifications.

where  $\mathcal{Z}_{n^{q-1}}^{(q)}$  is the partition function obtained by contracting  $n^{q-1}$  copies of the reduced density matrix with replica symmetry  $\mathbb{Z}_n^{\otimes(q-1)}$  as described above. See Fig. 1 for the graphical notation of the wavefunction and reduced density matrix, and Fig. 2 for the contractions of reduced density matrices at  $q = 3$ ,  $n = 2, 3$ . See also Fig. 3 for the generalization to quadripartite case with  $n = 2$ . Also note that when  $q = 2$ , Eq. (2.6) reduces to Rényi entropy. The multi-entropy is defined by taking the  $n \rightarrow 1$  limit

$$S^{(q)} = \lim_{n \rightarrow 1} S_n^{(q)} . \quad (2.7)$$

For  $q = 3$  and  $n = 2$ , the partition function contains 4 replicas with the gluing  $\sigma_B = (13)(24)$  and  $\sigma_C = (12)(34)$  as illustrated in Fig. 2. This results in a contraction of four density matrices (here we abbreviate  $\rho_{BC}$  as  $\rho$ )

$$\mathcal{Z}_{2^3-1}^{(3)} = \rho_{\beta_1 \chi_1}^{\beta_3 \chi_2} \rho_{\beta_2 \chi_2}^{\beta_4 \chi_1} \rho_{\beta_3 \chi_3}^{\beta_1 \chi_4} \rho_{\beta_4 \chi_4}^{\beta_2 \chi_3} . \quad (2.8)$$

The corresponding Rényi tri-entropy<sup>4</sup> is given by

$$S_2^{(3)}(A; B; C) = \frac{1}{1-2} \frac{1}{2^{3-2}} \log \left( \mathcal{Z}_{2^3-1}^{(3)} / (\mathcal{Z}_1^{(3)})^{2^{3-1}} \right) , \quad (2.9)$$

with  $\mathcal{Z}_1^{(3)} = \rho_{\beta \chi}^{\beta \chi}$  serving as the normalization factor.

## 2.2 Genuine Rényi tri-entropy

The genuine Rényi multi-entropy  $GM_n^{(q)}$  is constructed based on the Rényi multi-entropy (2.6) and the Rényi entropy (2.2). It satisfies the following two properties [16, 17]:

- $GM_n^{(q)}(A_1; A_2; \dots; A_q)$  is defined in terms of the  $q'$ -partite Rényi multi-entropy  $S_n^{(q')}$  with  $q' \leq q$ .
- $GM_n^{(q)}(A_1; A_2; \dots; A_q)$  vanishes for all states that can be factorized as

$$|\psi_q\rangle_{A_1 \dots A_q} = |\psi_{\tilde{q}}\rangle_{A'_1 \dots A'_{\tilde{q}}} \otimes |\psi_{q-\tilde{q}}\rangle_{A'_{\tilde{q}+1} \dots A'_q} , \quad (2.10)$$

where  $A'_i$  is a rearrangement of  $A_i$ , and  $\tilde{q} = 1, 2, \dots, q-1$ .

---

<sup>4</sup>In this paper, the tripartite/quadripartite multi-entropy is also called “tri/quadrupartite entropy”.

When  $q = 3$ , the genuine  $n$ -th Rényi tri-entropy is defined as [16, 17]

$$GM_n^{(3)}(A; B; C) = S_n^{(3)}(A; B; C) - \frac{1}{2}(S_n(A) + S_n(B) + S_n(C)) . \quad (2.11)$$

There are two typical tripartite entangled states, GHZ-state and W-state:

$$|\text{GHZ}_k^N\rangle = \sum_{i=0}^{k-1} \underbrace{|ii\cdots i\rangle}_N / \sqrt{k} , \quad (2.12)$$

$$|\text{W}^N\rangle = \left( \underbrace{|100\cdots 0\rangle}_N + |010\cdots 0\rangle + |001\cdots 0\rangle + \cdots \right) / \sqrt{N} . \quad (2.13)$$

We also consider the generalized GHZ-states and generalized W-states:

$$|\widetilde{\text{GHZ}}_k^N\rangle = \sum_{i=0}^{k-1} \lambda_i |ii\cdots i\rangle , \quad (2.14)$$

$$|\widetilde{\text{W}}^N\rangle = \cos \alpha |100\cdots 0\rangle + \sin \alpha \cos \beta |010\cdots 0\rangle + \sin \alpha \sin \beta \cos \chi |001\cdots 0\rangle + \cdots . \quad (2.15)$$

When  $n = 1$ , the genuine tri-entropy is believed to capture the intrinsic tripartite entanglement.<sup>5</sup> For the GHZ <sub>$k$</sub> -state (2.12),

$$GM_1^{(3)}[\text{GHZ}_k] = \frac{1}{2} \log k , \quad (2.16)$$

and for the generalized GHZ-states (2.14),  $GM_1^{(3)} \geq 0$ . Although we do not have a general proof that  $GM_1^{(3)}$  is always nonnegative, all the values of  $GM_1^{(3)}$  computed in this paper are indeed nonnegative.

When  $n = 2$ , the genuine Rényi tri-entropy can be interpreted as a symmetric version of the Markov gap. From the relation<sup>6</sup>

$$S_2^{(3)}(A; B; C) = \frac{1}{2} S_{2,2}^R(A; B) + S_2(AB) \quad (2.17)$$

between the second Rényi tri-entropy and the  $(m, n)$ -Rényi reflected entropy  $S_{m,n}^R(A; B)$  of subsystems  $A$  and  $B$  [11],<sup>7</sup> one finds that

$$\begin{aligned} GM_2^{(3)}(A; B; C) &= \frac{1}{2} S_{2,2}^R(A; B) + S_2(AB) - \frac{1}{2}(S_2(A) + S_2(B) + S_2(C)) \\ &= \frac{1}{2} \left[ S_{2,2}^R(A; B) - (S_2(A) + S_2(B) - S_2(AB)) \right] \\ &= \frac{1}{2} \left[ S_{2,2}^R(A; B) - I_2(A; B) \right] , \end{aligned} \quad (2.18)$$

where  $I_n(A; B) = S_n(A) + S_n(B) - S_n(AB)$  is the Rényi mutual information. The result in (2.18) closely resembles the definition of the Markov gap,

$$\Delta_n(A; B) = S_{1,n}^R(A; B) - I_n(A; B) , \quad (2.19)$$

<sup>5</sup>In the case of CFTs, the genuine tri-entropy is associated with the OPE coefficients of the corresponding twist operators [10].

<sup>6</sup>We use the notation  $AB$  to denote  $A \cup B$ .

<sup>7</sup>The relation (2.17) can be verified using the replica trick for these quantities.

evaluated at the Rényi index  $n = 2$ .

For the generalized W-state (2.15) with  $N = 3$ , the second genuine Rényi tri-entropy is nonnegative [18], and for the generalized GHZ-state (2.14),<sup>8</sup>

$$\text{GM}_2^{(3)}[\widetilde{\text{GHZ}}_k^N] \leq 0 . \quad (2.20)$$

### 2.3 Genuine Rényi quadri-entropy

The genuine Rényi quadri-entropy is defined as [16, 17]:

$$\begin{aligned} \text{GM}_n^{(4)}(A; B; C; D) := & S_n^{(4)}(A; B; C; D) \\ & - \frac{1}{3} \left( S_n^{(3)}(AB; C; D) + S_n^{(3)}(AC; B; D) + S_n^{(3)}(AD; B; C) \right. \\ & \quad \left. + S_n^{(3)}(BC; A; D) + S_n^{(3)}(BD; A; C) + S_n^{(3)}(CD; A; B) \right) \\ & + a \left( S_n(AB) + S_n(AC) + S_n(AD) \right) \\ & + \left( \frac{1}{3} - a \right) \left( S_n(A) + S_n(B) + S_n(C) + S_n(D) \right) , \end{aligned} \quad (2.21)$$

where  $a$  is a real free parameter. For GHZ <sub>$k$</sub> -state (2.12), we have [1]

$$S_n^{(q)}[\text{GHZ}_k] = \frac{n^{q-1} - 1}{(n-1)n^{q-2}} \log k . \quad (2.22)$$

Therefore, we have

$$\begin{aligned} \text{GM}_n^{(4)}[\text{GHZ}_k] &= \frac{\log k}{n-1} \left[ \frac{n^3 - 1}{n^2} - \frac{6}{3} \left( \frac{n^2 - 1}{n} \right) + 3a(n-1) + 4 \left( \frac{1}{3} - a \right) (n-1) \right] \\ &= \left( \frac{3 - 3n + n^2}{3n^2} - a \right) \log k . \end{aligned} \quad (2.23)$$

Note that when  $a = 1/12$ ,  $\text{GM}_2^{(4)}$  of the GHZ-state vanishes. One can also check that for the W-state (2.13) with  $N = 4$ , we have

$$\text{GM}_2^{(4)}[\text{W}^4] = a \log \frac{5^4}{2^9} + \log \frac{18}{5} - \frac{\log 5}{3} - \frac{\log 17}{4} , \quad (2.24)$$

which is positive when  $a = 1/12$ . Two other representative quadripartite entanglement patterns are the Cluster-state [28] and the Dicke-state [29],

$$|\text{Cluster}\rangle = \frac{1}{2} (|0000\rangle + |0011\rangle + |1100\rangle - |1111\rangle) , \quad (2.25)$$

$$|\text{Dicke}\rangle = \frac{1}{\sqrt{6}} (|0011\rangle + |0101\rangle + |0110\rangle + |1001\rangle + |1010\rangle + |1100\rangle) . \quad (2.26)$$

The  $n = 2$  genuine Rényi quadri-entropy for the Cluster-state (2.25) is

$$\text{GM}_2^{(4)}[\text{Cluster}] = \left( a - \frac{1}{12} \right) \log 2 , \quad (2.27)$$

which vanishes when  $a = 1/12$ . For the Dicke-state (2.26),

$$\text{GM}_2^{(4)}[\text{Dicke}] = \left( \frac{1}{12} - a \right) \log 2 - \frac{\log(3^7 \times 5 \times 11)}{4} + \log 19 , \quad (2.28)$$

which is positive when  $a = 1/12$ .

---

<sup>8</sup>See appendix A for a proof of (2.20).

### 3 Genuine multi-entropy for torus link states

#### 3.1 Multi-boundary states in Chern-Simons theory

We consider Chern-Simons theory with gauge group  $G$  at level  $k$ , whose action on a 3-manifold  $\mathcal{M}$  is

$$S_{\text{CS}}[A] = \frac{k}{4\pi} \int_{\mathcal{M}} \text{Tr} \left( A \wedge dA + \frac{2}{3} A \wedge A \wedge A \right), \quad (3.1)$$

with  $A$  the gauge field. In this paper we study a class of states called *link states*. These states are defined on  $\Sigma_N$ , which is the disjoint union of  $N$  copies of  $\mathbb{T}^2$ ,

$$\Sigma_N := \bigcup_{i=1}^N \mathbb{T}^2. \quad (3.2)$$

One can prepare these states by performing the Euclidean path integral of the theory (3.1) on a 3-manifold  $\mathcal{M}$  whose boundary is  $\Sigma_N$ . In this paper, we focus on the following construction. We start from  $\mathbb{S}^3$  containing a generic  $N$ -component link  $\mathcal{L}^N$ , which consists of  $N$  circles, i.e.,  $\mathcal{L}^N = \mathcal{C}_1 \cup \mathcal{C}_2 \cup \dots \cup \mathcal{C}_N$  (see the left part of Fig. 4). We then remove a tubular neighborhood of  $\mathcal{L}^N$  (middle part of Fig. 4), obtaining a 3-manifold denoted by  $\mathcal{M}_N = \mathbb{S}^3 \setminus \mathcal{L}^N$ , whose boundary is  $\Sigma_N$ . The construction for the case  $N = 3$  with  $\mathcal{L}^3 = 6_3^3$  is illustrated in Fig. 4.

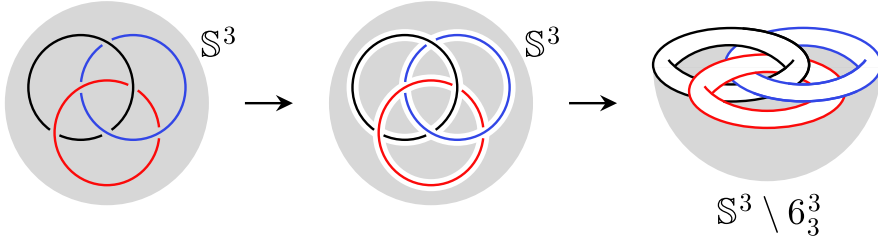


**Figure 4:** Figure showing the construction of link  $6_3^3$  complement. Removing a tubular neighborhood around link  $6_3^3$  embedded in  $\mathbb{S}^3$  results in link  $6_3^3$  complement which is a manifold with three torus boundaries. We note that the color in this figure (and Fig. 5) is used to distinguish different components and does not denote specific representation.

The wavefunction of the link state constructed in the above manner is given by [19]

$$|\mathcal{L}^N\rangle = \sum_{j_{1,2,\dots,N}} C_{\mathcal{L}^N}(j_1, j_2, \dots, j_N) |j_1, j_2, \dots, j_N\rangle, \quad (3.3)$$

where the complex coefficients  $C_{\mathcal{L}^N}(j_1, j_2, \dots, j_N)$  are the colored link invariants of Chern-Simons theory, with the representation  $R_{j_i}^*$  assigned to the  $i$ -th component of the link,

$$\begin{aligned} C_{\mathcal{L}^N}(j_1, j_2, \dots, j_N) &= \langle j_1, j_2, \dots, j_N | \mathcal{L}^N \rangle \\ &= \left\langle W_{R_{j_1}^*}(\mathcal{C}_1) W_{R_{j_2}^*}(\mathcal{C}_2) \cdots W_{R_{j_N}^*}(\mathcal{C}_N) \right\rangle. \end{aligned} \quad (3.4)$$

### 3.2 Abelian case

In this section, we focus on link states in  $U(1)_k$  Chern-Simons theory and study their genuine Rényi multi-entropies. For the three-component link case (Section 3.2.1), we obtain an analytical expression (3.25) valid for a general Rényi index  $n$ . For  $N$ -component links with  $N > 3$ , analytical results are available only for  $n = 2$ .

#### 3.2.1 Three-component links

For a generic three-component link  $\mathcal{L}^3$  in  $U(1)_k$  Chern-Simons theory, the corresponding normalized wavefunction can be expressed in terms of the colored link invariants [30]<sup>9</sup>

$$|\mathcal{L}^3\rangle = \frac{1}{k^{3/2}} \sum_{\alpha, \beta, \chi=0}^{k-1} e^{\frac{2\pi i}{k}(\alpha\beta L_{AB} + \beta\chi L_{BC} + \chi\alpha L_{CA})} |\alpha, \beta, \chi\rangle , \quad (3.5)$$

where  $\alpha$ ,  $\beta$ , and  $\chi$  denote the charges assigned to the loops  $A$ ,  $B$ , and  $C$ , respectively, and  $L_{AB}$  is the Gauss linking number between loops  $A$  and  $B$  (satisfying  $L_{AB} = L_{BA}$ ); similarly for  $L_{BC}$  and  $L_{CA}$ . The reduced density matrix  $\rho_{BC}$  is obtained by tracing out subsystem  $A$ , and its matrix elements are given by

$$\begin{aligned} \langle \beta, \chi | \rho_{BC} | \beta', \chi' \rangle &= \sum_{\alpha=0}^{k-1} \langle \alpha, \beta, \chi | \mathcal{L}^3 \rangle \langle \mathcal{L}^3 | \alpha, \beta', \chi' \rangle \\ &= \frac{1}{k^3} e^{\frac{2\pi i}{k}(\beta\chi - \beta'\chi')L_{BC}} \sum_{\alpha} e^{\frac{2\pi i}{k}\alpha((\beta - \beta')L_{AB} + (\chi - \chi')L_{CA})} \\ &= \frac{1}{k^2} e^{\frac{2\pi i}{k}(\beta\chi - \beta'\chi')L_{BC}} \eta[(\beta - \beta')L_{AB} + (\chi - \chi')L_{CA}] , \end{aligned} \quad (3.6)$$

where we have introduced the  $\eta$ -constraint function,<sup>10</sup>

$$\eta[x] = \frac{1}{k} \sum_{\alpha=0}^{k-1} e^{\frac{2\pi i}{k}\alpha x} = \begin{cases} 1 , & \text{if } x \equiv 0 \pmod{k} , \\ 0 , & \text{otherwise.} \end{cases} \quad (3.7)$$

The  $\eta$ -constraint function (3.7) satisfies the following properties:

$$\eta[x] = \eta[-x] , \quad \eta[x]^2 = \eta[x] , \quad \eta[x] \eta[y] = \eta[x+y] \eta[x] . \quad (3.8)$$

With the reduced density matrix (3.6), the second Rényi multi-entropy among  $A$ ,  $B$ , and  $C$  can be computed from its definitions (2.8) and (2.9). We first evaluate the partition function on the replica space using (2.8),

$$\begin{aligned} \mathcal{Z}_4^{(3)} &= \frac{1}{k^8} \sum_{\beta_1 \sim 4, \chi_1 \sim 4} \left\{ \exp \left[ \frac{2\pi i}{k} ((\beta_1 - \beta_4)(\chi_1 - \chi_4) + (\beta_2 - \beta_3)(\chi_2 - \chi_3)) L_{BC} \right] \right. \\ &\quad \times \eta[(\beta_1 - \beta_3)L_{AB} + (\chi_1 - \chi_2)L_{CA}] \eta[(\beta_2 - \beta_4)L_{AB} + (\chi_2 - \chi_1)L_{CA}] \\ &\quad \left. \times \eta[(\beta_3 - \beta_1)L_{AB} + (\chi_3 - \chi_4)L_{CA}] \eta[(\beta_4 - \beta_2)L_{AB} + (\chi_4 - \chi_3)L_{CA}] \right\} , \end{aligned} \quad (3.9)$$

<sup>9</sup>The  $U(1)_k$  Chern-Simons link states (3.5) and (3.27) are also called *weighted graph states*. See [31–33] for graph states on qubits and [34, 35] for  $k$ -bits.

<sup>10</sup>The notation  $x \equiv y \pmod{k}$  denotes that the two integers  $x$  and  $y$  are congruent modulo  $k$ .

which is a sum of terms of the form  $e^{(\dots)}/k^8$  over  $\beta_{1,2,3,4}$  and  $\chi_{1,2,3,4}$ , subject to the constraints imposed by the  $\eta$ -functions. To handle these  $\eta$ -constraints, note that, for example,  $\eta[(\beta_1 - \beta_3)L_{AB} + (\chi_1 - \chi_2)L_{CA}]$  is a function of<sup>11</sup>

$$\beta_{13} := (\beta_1 - \beta_3) \bmod k \quad \text{and} \quad \chi_{12} := (\chi_1 - \chi_2) \bmod k . \quad (3.10)$$

Therefore, we can make the following change of variables

$$\beta_3 \rightarrow \beta_1 - \beta_{13} , \quad \beta_4 \rightarrow \beta_2 - \beta_{24} , \quad \chi_2 \rightarrow \chi_1 - \chi_{12} , \quad \chi_4 \rightarrow \chi_3 - \chi_{34} \quad (3.11)$$

in (3.9) and obtain

$$\begin{aligned} z_4^{(3)} = \frac{1}{k^8} \sum_{\beta_{1,2,13,24}, \chi_{1,3,12,34}} & \left\{ \exp \left[ \frac{2\pi i}{k} (-\beta_{13}\chi_{12} + \beta_{24}\chi_{34})L_{BC} \right] \right. \\ & \times \exp \left[ \frac{2\pi i}{k} \beta_1(\chi_{12} + \chi_{34})L_{BC} \right] \exp \left[ \frac{2\pi i}{k} \beta_2(-\chi_{12} - \chi_{34})L_{BC} \right] \\ & \times \exp \left[ \frac{2\pi i}{k} \chi_1(\beta_{13} + \beta_{24})L_{BC} \right] \exp \left[ \frac{2\pi i}{k} \chi_3(-\beta_{13} - \beta_{24})L_{BC} \right] \\ & \times \eta[\beta_{13}L_{AB} + \chi_{12}L_{CA}] \eta[\beta_{24}L_{AB} - \chi_{12}L_{CA}] \\ & \left. \times \eta[-\beta_{13}L_{AB} + \chi_{34}L_{CA}] \eta[-\beta_{24}L_{AB} - \chi_{34}L_{CA}] \right\} . \end{aligned} \quad (3.12)$$

Since  $\beta_{1,2}$  and  $\chi_{1,3}$  do not appear in the  $\eta$ -constraints in (3.12), we can sum them using (3.7) and end up with a summation over  $\beta_{13,24}, \chi_{12,34}$  of

$$\frac{1}{k^4} \exp \left[ \frac{2\pi i}{k} (-\beta_{13}\chi_{12} + \beta_{24}\chi_{34})L_{BC} \right] \quad (3.13)$$

with the following constraints

$$\begin{aligned} 1 = & \eta[(\chi_{12} + \chi_{34})L_{BC}] \eta[(-\chi_{12} - \chi_{34})L_{BC}] \eta[(\beta_{13} + \beta_{24})L_{BC}] \eta[(-\beta_{13} - \beta_{24})L_{BC}] \\ & \times \eta[\beta_{13}L_{AB} + \chi_{12}L_{CA}] \eta[\beta_{24}L_{AB} - \chi_{12}L_{CA}] \\ & \times \eta[-\beta_{13}L_{AB} + \chi_{34}L_{CA}] \eta[-\beta_{24}L_{AB} - \chi_{34}L_{CA}] . \end{aligned} \quad (3.14)$$

Among them, the constraints  $1 = \eta[(\chi_{12} + \chi_{34})L_{BC}]$  and  $1 = \eta[(\beta_{13} + \beta_{24})L_{BC}]$  force

$$\exp \left[ \frac{2\pi i}{k} (-\beta_{13}\chi_{12} + \beta_{24}\chi_{34})L_{BC} \right] = 1 . \quad (3.15)$$

Therefore, the summation reduces to finding out how many sets of  $(\beta_{13,24}, \chi_{12,34}) \in \mathbb{Z}_k^{\otimes 4}$  can survive under the constraint (3.14). To figure this out, we first use the properties in (3.8) to simplify (3.14) to

$$\begin{aligned} 1 = & \eta[(\chi_{12} + \chi_{34})L_{BC}] \eta[(\beta_{13} + \beta_{24})L_{BC}] \\ & \times \eta[(\beta_{13} + \beta_{24})L_{AB}] \eta[(\chi_{12} + \chi_{34})L_{CA}] \eta[\beta_{13}L_{AB} + \chi_{12}L_{CA}] . \end{aligned} \quad (3.16)$$

---

<sup>11</sup>We use the notation “:=” to denote a definition.

Performing the change of variables

$$\beta_{24} \rightarrow b - \beta_{13} , \quad \chi_{34} \rightarrow c - \chi_{12} ,$$

(3.16) is further simplified to

$$1 = \eta[c L_{BC}] \eta[c L_{CA}] \eta[b L_{BC}] \eta[b L_{AB}] \eta[\beta_{13} L_{AB} + \chi_{12} L_{CA}] . \quad (3.17)$$

Now we can count the number of solutions. There are (“gcd” denotes the greatest common divisor)

- $\gcd(k, L_{AB}, L_{BC})$  possible  $b \in \mathbb{Z}_k$  satisfying  $1 = \eta[b L_{BC}] \eta[b L_{AB}]$ ,
- $\gcd(k, L_{BC}, L_{CA})$  possible  $c \in \mathbb{Z}_k$  satisfying  $1 = \eta[c L_{BC}] \eta[c L_{CA}]$ ,
- $k \cdot \gcd(k, L_{CA}, L_{AB})$  possible  $\{\beta_{13}, \chi_{12}\} \in \mathbb{Z}_k^{\otimes 2}$  satisfying  $1 = \eta[\beta_{13} L_{AB} + \chi_{12} L_{CA}]$ .<sup>12</sup>

Therefore, we obtain

$$\begin{aligned} \mathcal{Z}_4^{(3)} &= k^{-3} \gcd(k, L_{CA}, L_{AB}) \gcd(k, L_{AB}, L_{BC}) \gcd(k, L_{BC}, L_{CA}) \\ \Rightarrow S_2^{(3)}(A; B; C) &= \frac{1}{2} \log \frac{k^3}{\gcd(k, L_{CA}, L_{AB}) \gcd(k, L_{AB}, L_{BC}) \gcd(k, L_{BC}, L_{CA})} . \end{aligned} \quad (3.18)$$

One can see that the key idea is to use the variable substitution together with (3.7) to generate as many constraints as possible, so that the summand becomes 1, thereby reducing the problem to counting the number of solutions that satisfy all the constraints. However, this task becomes difficult when the Rényi index  $n > 2$ . Nevertheless, if one of the three linking numbers is set to zero, the problem can be solved (without loss of generality, we set  $L_{BC} = 0$  here),

$$S_n^{(3)}(A; B; C)|_{L_{BC}=0} = \frac{1}{n} \log \frac{k^{n+1}}{\gcd(k, L_{CA}, L_{AB})^{n-1} \gcd(k, L_{AB}) \gcd(k, L_{CA})} \quad (3.19)$$

$$= \frac{1}{n} \log \frac{k^3}{\gcd(k, L_{CA}, L_{AB}) \gcd(k, L_{AB}) \gcd(k, L_{CA})} \quad (3.20)$$

$$+ \left(1 - \frac{2}{n}\right) \log \frac{k}{\gcd(k, L_{CA}, L_{AB})} . \quad (3.21)$$

We leave the tedious derivation of (3.19) to Appendix B. We now aim to obtain a complete result for  $L_{BC} \neq 0$ , based on the  $n = 2$  result (3.18) and the general- $n$ ,  $L_{BC} = 0$  result (3.19). By comparing (3.20) with (3.18) and recalling that  $L_{BC} = 0$ , we are led to perform the following improvements in (3.20):

$$\begin{aligned} \gcd(k, L_{AB}) &= \gcd(k, L_{AB}, 0) \rightarrow \gcd(k, L_{AB}, L_{BC}) , \\ \gcd(k, L_{CA}) &= \gcd(k, 0, L_{CA}) \rightarrow \gcd(k, L_{BC}, L_{CA}) . \end{aligned} \quad (3.22)$$

---

<sup>12</sup>See footnote 3 of [19].

By symmetry among  $L_{AB}$ ,  $L_{BC}$ , and  $L_{CA}$ , the term  $\gcd(k, L_{CA}, L_{AB})$  in (3.21) should be replaced with  $\gcd(k, L_{CA}, L_{AB}, L_{BC})$ . This leads to a formula for the  $n$ -th Rényi multi-entropy of three-component links with linking numbers  $L_{AB}, L_{BC}, L_{CA}$

$$S_n^{(3)}(A; B; C) = \frac{1}{n} \log \frac{k^3}{\gcd(k, L_{CA}, L_{AB}) \gcd(k, L_{AB}, L_{BC}) \gcd(k, L_{BC}, L_{CA})} + \left(1 - \frac{2}{n}\right) \log \frac{k}{\gcd(k, L_{CA}, L_{AB}, L_{BC})} . \quad (3.23)$$

We emphasize that the formula (3.23) above is a conjecture, based on the rigorous results (3.18) and (3.19). Nevertheless, it has been confirmed by extensive numerical checks.<sup>13</sup>

The  $n$ -th Rényi entropy  $S_n(A; BC)$  for the wavefunction (3.5) is given by [19]

$$S_n(A; BC) = \log \frac{k}{\gcd(k, L_{CA}, L_{AB})} , \quad (3.24)$$

from which it follows that the genuine Rényi multi-entropy (2.11) of the three-component link state (3.5) is

$$\text{GM}_n^{(3)}(A; B; C) = \left(\frac{1}{n} - \frac{1}{2}\right) \log \frac{k \cdot \gcd(k, L_{CA}, L_{AB}, L_{BC})^2}{\gcd(k, L_{CA}, L_{AB}), \gcd(k, L_{AB}, L_{BC}), \gcd(k, L_{BC}, L_{CA})} . \quad (3.25)$$

In Appendix E, we prove the following inequality using a Venn diagram:

$$1 \leq \frac{k \cdot \gcd(k, L_{CA}, L_{AB}, L_{BC})^2}{\gcd(k, L_{CA}, L_{AB}), \gcd(k, L_{AB}, L_{BC}), \gcd(k, L_{BC}, L_{CA})} \leq k , \quad (3.26)$$

from which it is clear that the logarithmic term in (3.25) is nonnegative and bounded above by  $\log k$ .

### 3.2.2 $N$ -component links

The calculation in Section 3.2.1 can be directly generalized to  $N$ -component links<sup>14</sup> and we present only an abbreviated derivation. We divide the  $N$  loops into three groups,  $\{A_1, A_2, \dots, A_{N_A}\}$ ,  $\{B_1, B_2, \dots, B_{N_B}\}$  and  $\{C_1, C_2, \dots, C_{N_C}\}$ , with  $L_{A_i B_j}$ ,  $L_{B_i C_j}$  and  $L_{C_i A_j}$  the corresponding Gauss linking numbers between different groups<sup>15</sup>. The wavefunction is

$$|\mathcal{L}^N\rangle = \frac{1}{k^{N/2}} \sum_{\alpha_i, \beta_j, \chi_k=0}^{k-1} e^{\frac{2\pi i}{k} \sum_{i,j} (\alpha_i \beta_j L_{A_i B_j} + \beta_i \chi_j L_{B_i C_j} + \chi_i \alpha_j L_{C_i A_j} + \dots)} |\{\alpha_i\}, \{\beta_j\}, \{\chi_k\}\rangle . \quad (3.27)$$

The second Rényi multi-entropy can be computed similarly:

$$S_2^{(3)}(A; B; C) = \frac{1}{2} \log \frac{k^N}{|\ker G_{BC,A}| \cdot |\ker G_{CA,B}| \cdot |\ker G_{AB,C}|} , \quad (3.28)$$

<sup>13</sup>We numerically verified (3.23) for  $n = 3$  for all three-component links with  $k \leq 17$ , for  $n = 4$  with  $k \leq 6$ , for  $n = 5$  with  $k \leq 5$ , and for  $n = 6$  with  $k \leq 4$ .

<sup>14</sup>Here,  $N$  denotes the number of components, while  $n$  always refers to the Rényi index.

<sup>15</sup>There can be non-trivial linking numbers between loops in the same group like  $L_{A_i A_j}$ . However, both the Rényi multi-entropy and the Rényi entropy do not depend on them [21]. Therefore, we do not explicitly include terms such as  $\alpha_i \alpha_j L_{A_i A_j}$  in (3.27).

where  $G_{BC,A}$  is a  $(N_B + N_C) \times N_A$ -matrix called linking matrix

$$G_{BC,A} = \begin{pmatrix} L_{B_1 A_1} & L_{B_1 A_2} & \cdots & L_{B_1 A_{N_A}} \\ \vdots & \vdots & \ddots & \vdots \\ L_{B_{N_B} A_1} & L_{B_{N_B} A_2} & \cdots & L_{B_{N_B} A_{N_A}} \\ L_{C_1 A_1} & L_{C_1 A_2} & \cdots & L_{C_1 A_{N_A}} \\ \vdots & \vdots & \ddots & \vdots \\ L_{C_{N_C} A_1} & L_{C_{N_C} A_2} & \cdots & L_{C_{N_C} A_{N_A}} \end{pmatrix} \quad (3.29)$$

and  $|\ker G_{BC,A}|$  denotes the number of solutions  $\vec{x} \in \mathbb{Z}_k^{\otimes N_A}$  to the congruence equations

$$G_{BC,A} \cdot \vec{x} \equiv 0 \pmod{k} . \quad (3.30)$$

The  $n$ -th Rényi entropy  $S_n(A; BC)$  for this general  $N$ -component link is given by [19],

$$S_n(A; BC) = \log \frac{k^{N_A}}{|\ker G_{BC,A}|} . \quad (3.31)$$

One can see that for  $N$ -links,  $\text{GM}_2^{(3)}$  vanishes just as in the three-component case (3.25).<sup>16</sup>

### 3.2.3 Quadri-entropy of four-component links

We also compute  $S_2^{(4)}(A; B; C; D)$  using the method described in Section 3.2.1:

$$\begin{aligned} S_2^{(4)}(A; B; C; D) &= \frac{1}{4} \log \frac{k^4}{|\ker G_{BCD,A}| \cdot |\ker G_{CDA,B}| \cdot |\ker G_{DAB,C}| \cdot |\ker G_{ABC,D}|} \\ &\quad + \frac{1}{4} \log \frac{k^6}{|\ker G_{AB,CD}| \cdot |\ker G_{AC,BD}| \cdot |\ker G_{AD,BC}|} \\ &= \frac{1}{4} \left( S_2(A) + S_2(B) + S_2(C) + S_2(D) + S_2(AB) + S_2(AC) + S_2(AD) \right) . \end{aligned} \quad (3.32)$$

One can check that if  $a = 1/12$ , the corresponding second genuine Rényi quadri-entropy  $\text{GM}_2^{(4)}$  (2.21) vanishes, similar to the second genuine Rényi tri-entropy  $\text{GM}_2^{(3)}$  case (3.25), implying that four-link states contain only GHZ-type and Cluster-type quadripartite entanglement (see the results (2.23), (2.24), (2.27) and (2.28) in Section 2.3).

## 3.3 Non-Abelian case

In this section, we focus on  $\text{SU}(2)_k$  Chern-Simons theory. We consider three-component links (see Fig. 5) and compute the genuine tri-entropy among the components.

---

<sup>16</sup>In this paper we sometimes abbreviate “ $N$ -component link” as “ $N$ -link”.

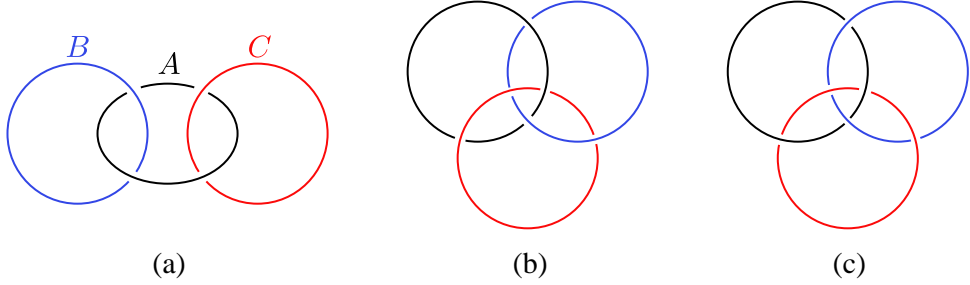


**Figure 5:** (a) The connected sum of two Hopf links (the link  $2_1^2 + 2_1^2$ ). (b) The link  $6_3^3$ . (c) Borromean rings (the link  $6_2^3$ ).

### 3.3.1 Connected sum of two Hopf links

We start with the link  $2_1^2 + 2_1^2$ , which is the connected sum of two Hopf links (see Fig. 5 (a)). By evaluating the link invariant in Eq. (3.4), one obtains the wavefunction of this link [19]

$$|2_1^2 + 2_1^2\rangle = \sum_{\alpha, \beta, \chi, m} S_{\alpha m} N_{m \beta \chi} |\alpha, \beta, \chi\rangle = \sum_{\alpha, \beta, \chi} \frac{S_{\beta \alpha} S_{\chi \alpha}}{S_{0 \alpha}} |\alpha, \beta, \chi\rangle , \quad (3.33)$$

where the spins  $\alpha = 0, \frac{1}{2}, \dots, \frac{k}{2}$  label the integrable representations of  $SU(2)_k$ ,  $N_{m \beta \chi}$  denotes the fusion coefficients, and at the second equal sign we have applied the Verlinde formula

$$N_{m \beta \chi} = \sum_j \frac{S_{mj} S_{\beta j} S_{\chi j}}{S_{0j}} \quad (3.34)$$

and the property

$$S_{\alpha m} S_{mj} = S_{\bar{\alpha} m}^* S_{mj} = \delta_{\bar{\alpha} j} \quad (3.35)$$

of the  $S$ -matrix<sup>17</sup>. The reduced density matrix is given by<sup>18</sup>

$$\langle \beta, \chi | \rho_{BC} | \beta', \chi' \rangle = \sum_{\alpha} \frac{S_{\beta \alpha} S_{\chi \alpha}}{S_{0 \alpha}} \frac{S_{\beta' \alpha}^* S_{\chi' \alpha}^*}{S_{0 \alpha}^*} . \quad (3.37)$$

Using (2.8), we get (repeated indices in the following expression are to be summed over)

$$\begin{aligned} \mathcal{Z}_4^{(3)} = & \frac{S_{\beta_1 \alpha_1} S_{\chi_1 \alpha_1}}{S_{0 \alpha_1}} \frac{S_{\beta_3 \alpha_1}^* S_{\chi_2 \alpha_1}^*}{S_{0 \alpha_1}^*} \frac{S_{\beta_2 \alpha_2} S_{\chi_2 \alpha_2}}{S_{0 \alpha_2}} \frac{S_{\beta_4 \alpha_2}^* S_{\chi_1 \alpha_2}^*}{S_{0 \alpha_2}^*} \\ & \times \frac{S_{\beta_3 \alpha_3} S_{\chi_3 \alpha_3}}{S_{0 \alpha_3}} \frac{S_{\beta_1 \alpha_3}^* S_{\chi_4 \alpha_3}^*}{S_{0 \alpha_3}^*} \frac{S_{\beta_4 \alpha_4} S_{\chi_4 \alpha_4}}{S_{0 \alpha_4}} \frac{S_{\beta_2 \alpha_4}^* S_{\chi_3 \alpha_4}^*}{S_{0 \alpha_4}^*} \end{aligned} \quad (3.38)$$

<sup>17</sup>The specific form of the  $SU(2)_k$   $S$ -matrix is

$$S_{\alpha \beta} = \sqrt{\frac{2}{k+2}} \sin\left(\frac{(2\alpha+1)(2\beta+1)\pi}{k+2}\right) . \quad (3.36)$$

<sup>18</sup>Note that the reduced density matrix  $\rho_{BC}$  in (3.37) is unnormalized,  $\text{Tr} \rho_{BC} = \sum_{\alpha} |S_{0 \alpha}|^{-2} = \sum_{\alpha} \mathcal{D}^2 / d_{\alpha}^2$ .

Using the property (3.35) of  $S$ -matrix repeatedly, one can sum over  $\beta_{1,2,3,4}$ ,  $\chi_{1,2,3,4}$  and end up with  $\delta$ -functions

$$\begin{aligned}\mathcal{Z}_4^{(3)} &= \frac{\delta_{\alpha_1 \alpha_3} \delta_{\alpha_1 \alpha_2}}{S_{0 \alpha_1}} \frac{\delta_{\alpha_1 \alpha_3} \delta_{\alpha_1 \alpha_2}}{S_{0 \alpha_1}^*} \frac{\delta_{\alpha_2 \alpha_4}}{S_{0 \alpha_2}} \frac{\delta_{\alpha_2 \alpha_4}}{S_{0 \alpha_2}^*} \frac{\delta_{\alpha_3 \alpha_4}}{S_{0 \alpha_3}} \frac{\delta_{\alpha_3 \alpha_4}}{S_{0 \alpha_3}^*} \frac{1}{S_{0 \alpha_4}} \frac{1}{S_{0 \alpha_4}^*} \\ &= \sum_{\alpha} |S_{0 \alpha}|^{-8} = \sum_{\alpha} \mathcal{D}^8 / d_{\alpha}^8 \\ \Rightarrow S_2^{(3)}(A; B; C) &= -\frac{1}{2} \log \frac{\sum_{\alpha} \mathcal{D}^8 / d_{\alpha}^8}{(\sum_{\alpha} \mathcal{D}^2 / d_{\alpha}^2)^4} = \frac{1}{2} \log \frac{(\sum_{\alpha} d_{\alpha}^{-2})^4}{\sum_{\alpha} d_{\alpha}^{-8}} ,\end{aligned}\quad (3.39)$$

where in the second line we sum over  $\alpha_{2,3,4}$  and rename  $\alpha_1$  as  $\alpha$ . In the final result,  $d_{\alpha}$  is the quantum dimension of anyon  $\alpha$  and

$$\mathcal{D} = \sqrt{\sum_{\alpha} d_{\alpha}^2} \quad (3.40)$$

is the total quantum dimension.

One can calculate the  $n$ -th Rényi multi-entropy similarly, and the result is

$$\begin{aligned}\mathcal{Z}_{n^2}^{(3)} &= \sum_{\alpha} |S_{0 \alpha}|^{-2n^2} = \sum_{\alpha} \mathcal{D}^{2n^2} / d_{\alpha}^{2n^2} \\ \Rightarrow S_n^{(3)}(A; B; C) &= \frac{1}{1-n} \frac{1}{n} \log \frac{\sum_{\alpha} \mathcal{D}^{2n^2} / d_{\alpha}^{2n^2}}{(\sum_{\alpha} \mathcal{D}^2 / d_{\alpha}^2)^{n^2}} = \frac{\log (\sum_{\alpha} p_{\alpha}^{n^2})}{(1-n)n} , \quad p_{\alpha} = \frac{d_{\alpha}^{-2}}{\sum_j d_j^{-2}} .\end{aligned}\quad (3.41)$$

In the  $n \rightarrow 1$  limit, we have

$$\begin{aligned}S_1^{(3)}(A; B; C) &= \lim_{n \rightarrow 1} \frac{1}{n-1} \left[ \log \frac{(\sum_{\alpha} d_{\alpha}^{-2})^{n^2}}{\sum_{\alpha} d_{\alpha}^{-2n^2}} - \log \frac{\sum_{\alpha} d_{\alpha}^{-2}}{\sum_{\alpha} d_{\alpha}^{-2}} + \log \frac{\sum_{\alpha} d_{\alpha}^{-2}}{\sum_{\alpha} d_{\alpha}^{-2}} \right] \\ &= \lim_{n \rightarrow 1} \frac{\partial}{\partial n} \log \frac{(\sum_{\alpha} d_{\alpha}^{-2})^{n^2}}{\sum_{\alpha} d_{\alpha}^{-2n^2}} \\ &= -2 \sum_{\alpha} p_{\alpha} \log p_{\alpha} .\end{aligned}\quad (3.42)$$

The  $n$ -th Rényi entropy of the state (3.33) is [19]

$$S_n(AB; C) = S_n(BC; A) = S_n(CA; B) = \frac{\log (\sum_{\alpha} p_{\alpha}^n)}{1-n} .\quad (3.43)$$

In the  $n \rightarrow 1$  limit, we have

$$S_1(AB; C) = S_1(BC; A) = S_1(CA; B) = - \sum_{\alpha} p_{\alpha} \log p_{\alpha} .\quad (3.44)$$

Therefore, the genuine multi-entropy (2.11) of the state (3.33) is

$$GM_1^{(3)}(A; B; C) = -\frac{1}{2} \sum_{\alpha} p_{\alpha} \log p_{\alpha} .\quad (3.45)$$

Note also that this genuine multi-entropy is positive and bounded from above by  $\frac{1}{2} \log(k+1)$ .

We plot the data for the second genuine Rényi multi-entropy of this link in Fig. 6 for  $SU(2)_k$  Chern-Simons theory. It can be seen that the  $GM_2^{(3)}$  among the three loops is always negative, indicating that the state (3.33) is GHZ-like (according to (2.20)).

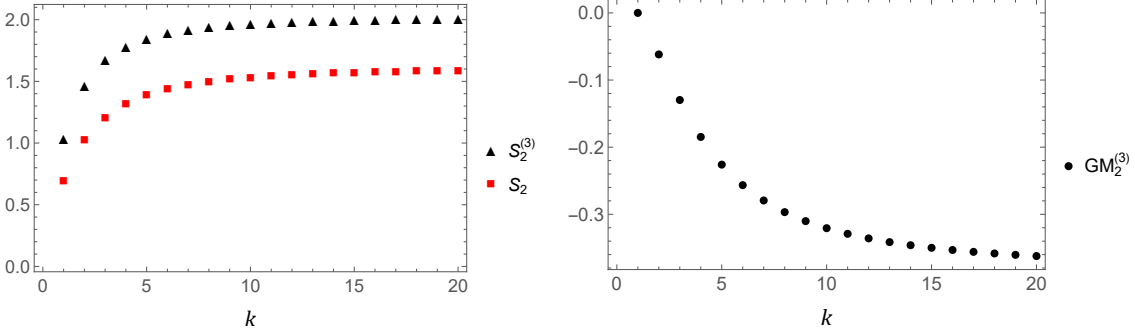


**Figure 6:** (Left) The second Rényi multi-entropy (3.39) and second Rényi entropy (3.43) for the link  $2_1^2 + 2_1^2$  as a function of  $k$ . (Right) The second genuine Rényi multi-entropy for  $2_1^2 + 2_1^2$  as a function of  $k$ .

### 3.3.2 Link $6_3^3$

The link  $6_3^3$  (Fig. 5 (b)) differs from the link  $2_1^2 + 2_1^2$  by a Dehn twist between  $B$  and  $C$ , thus its wavefunction is [19]

$$|6_3^3\rangle = \sum_{\alpha, \beta, \chi} \sum_m e^{-2\pi i(h_m + h_\alpha + h_\beta + h_\chi)} \frac{S_{\alpha m} S_{\beta m} S_{\chi m}}{S_{0m}} |\alpha, \beta, \chi\rangle , \quad (3.46)$$

where  $h_\alpha = \alpha(\alpha + 1)/(k + 2)$  is related to the  $\mathcal{T}$ -matrix through  $\mathcal{T}_{\alpha\beta} = e^{2\pi i h_\alpha} \delta_{\alpha\beta}$ . The reduced density matrix is given by

$$\begin{aligned} \langle \beta, \chi | \rho_{BC} | \beta', \chi' \rangle &= \sum_{\alpha} \sum_{m, n} e^{-2\pi i(h_m - h_n + h_\beta - h_{\beta'} + h_\chi - h_{\chi'})} \frac{S_{\alpha m} S_{\beta m} S_{\chi m}}{S_{0m}} \frac{S_{\alpha n}^* S_{\beta' n}^* S_{\chi' n}^*}{S_{0n}^*} \\ &= e^{-2\pi i(h_\beta - h_{\beta'} + h_\chi - h_{\chi'})} \sum_m \frac{S_{\beta m} S_{\chi m}}{S_{0m}} \frac{S_{\beta' m}^* S_{\chi' m}^*}{S_{0m}^*} . \end{aligned} \quad (3.47)$$

In the second line of (3.47), we use the property (3.35). One can see that the result in (3.47) is almost identical to (3.37), up to a phase factor that cancels when computing the partition function on the replica space (2.8). Therefore, the  $n$ -th Rényi multi-entropy among the three loops of the  $6_3^3$  link is exactly the same as that in (3.41). We also note that the second Rényi entropy of the state (3.46) coincides with (3.43) [19].

### 3.3.3 Borromean rings

A more complicated link is the Borromean rings  $6_2^3$  (Fig. 5 (c)), whose wavefunction is given by [19]

$$|6_2^3\rangle = \sum_{j=0}^{\min(\alpha, \beta, \chi)} (-1)^j (q^{1/2} - q^{-1/2})^{4j} \frac{[2\alpha + j + 1]! [2\beta + j + 1]! [2\chi + j + 1]! ([j]!)^2}{[2\alpha - j]! [2\beta - j]! [2\chi - j]! ([2j + 1]!)^2} |\alpha, \beta, \chi\rangle , \quad (3.48)$$

with

$$[x] = \frac{q^{x/2} - q^{-x/2}}{q^{1/2} - q^{-1/2}} , \quad [x]! = [x][x-1] \cdots [1] , \quad q = e^{2\pi i/(k+2)} . \quad (3.49)$$

For this state, we do not have an analytic formula for  $S_n^{(3)}$ . The numerical results for  $S_2$ ,  $S_2^{(3)}$ , and  $\text{GM}_2^{(3)}$  are plotted in Fig. 7.

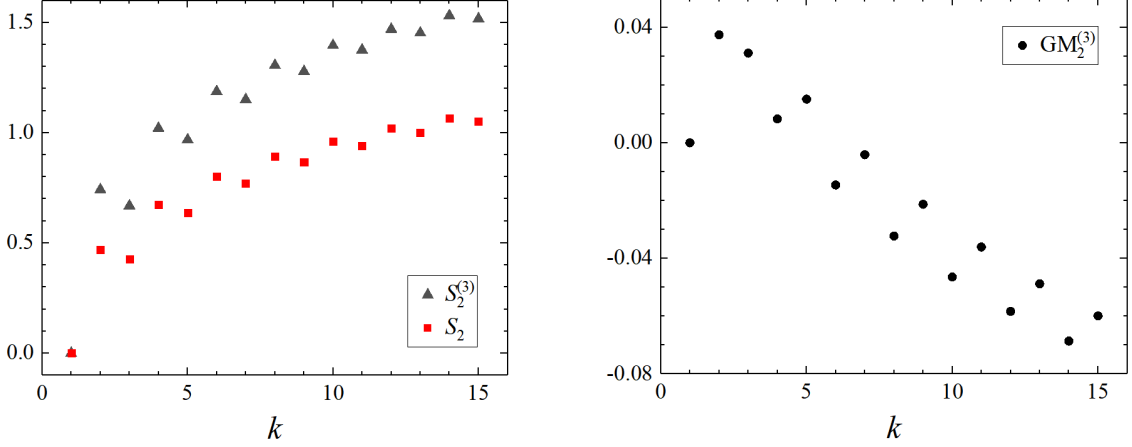


**Figure 7:** (Left) The second Rényi multi-entropy and second Rényi entropy for the Borromean link as a function of  $k$ . (Right) The second genuine Rényi multi-entropy for the Borromean link as a function of  $k$ .

#### 4 Logarithmic negativity for three-component links

Logarithmic negativity [36, 37] is a readily computable measure of bipartite quantum entanglement that applies to both pure and mixed states. The logarithmic negativity between subsystems  $B$  and  $C$  is defined as

$$E_N(B; C) = \log \|\rho_{BC}^\Gamma\|, \quad (4.1)$$

where  $\|O\| = \text{Tr}\sqrt{O^\dagger O}$  is the trace norm of the matrix  $O$ , and  $\rho_{BC}^\Gamma$  denotes the partial transpose of the reduced density matrix  $\rho_{BC}$

$$\langle \beta, \chi | \rho_{BC}^\Gamma | \beta', \chi' \rangle = \langle \beta, \chi' | \rho_{BC} | \beta', \chi \rangle. \quad (4.2)$$

A non-zero logarithmic negativity strictly signals the presence of pure quantum entanglement. It serves as an effective entanglement witness, consistently identifying entangled states and exclusively measuring quantum correlations, without including classical correlations.

The logarithmic negativity can also be computed using the replica trick, in close analogy to the entanglement entropy. The trace norm of the partially transposed density matrix can be expressed in terms of its eigenvalues,

$$\text{Tr} \|\rho_{BC}^\Gamma\| = 1 + 2 \sum_{\lambda_i < 0} |\lambda_i|. \quad (4.3)$$

Therefore, one can recover the trace norm by analytically continuing the even integer powers of the partially transposed density matrix

$$\text{Tr} (\rho_{BC}^\Gamma)^{2p} = \sum_i \lambda_i^{2p}, \quad p \in \mathbb{Z}_+. \quad (4.4)$$

to  $p = 1/2$ , i.e.,

$$E_N(B; C) = \lim_{p \rightarrow 1/2} \log \text{Tr}(\rho_{BC}^\Gamma)^{2p}. \quad (4.5)$$

From (3.6), the partial transpose of the reduced density matrix for a three-component link state is

$$\langle \beta, \chi | \rho_{BC}^\Gamma | \beta', \chi' \rangle = \frac{1}{k^2} e^{\frac{2\pi i}{k} (\beta\chi' - \beta'\chi)L_{BC}} \eta[(\beta - \beta')L_{AB} - (\chi - \chi')L_{CA}]. \quad (4.6)$$

When  $p = 1$ , we have

$$\begin{aligned} \text{Tr}(\rho_{BC}^\Gamma)^2 &= \sum_{\beta_{1,2}, \chi_{1,2}} \frac{1}{k^4} \eta[(\beta_1 - \beta_2)L_{AB} - (\chi_1 - \chi_2)L_{CA}] \eta[(\beta_2 - \beta_1)L_{AB} - (\chi_2 - \chi_1)L_{CA}] \\ &= \frac{1}{k^4} \times k^2 \times k \text{gcd}(k, L_{CA}, L_{AB}) \\ &= \frac{1}{k} \text{gcd}(k, L_{CA}, L_{AB}), \end{aligned} \quad (4.7)$$

where in the second line, the factor  $k \text{gcd}(k, L_{CA}, L_{AB})$  arises from the fact that there are  $k \text{gcd}(k, L_{CA}, L_{AB})$  sets of  $\{\beta_1 - \beta_2, \chi_1 - \chi_2\}$  satisfying the  $\eta$ -constraint, while the factor  $k^2$  comes from the two free variables. For  $p > 1$ , it is difficult to perform a similar calculation. Nevertheless, we can first obtain the result for  $L_{CA} = 0$  (see appendix C for the derivation)

$$\text{Tr}(\rho_{BC}^\Gamma)^{2p} \Big|_{L_{CA}=0} = \frac{1}{k^{2p-1}} \text{gcd}(k, L_{AB}, L_{BC})^{2p-2} \text{gcd}(k, L_{AB}). \quad (4.8)$$

A complete result with nontrivial  $L_{CA}$  should reduce to (4.7) when  $p = 1$ , and should be symmetric between  $B$  and  $C$ . Therefore, we make the following improvement

$$\text{gcd}(k, L_{AB}) = \text{gcd}(k, 0, L_{AB}) \rightarrow \text{gcd}(k, L_{CA}, L_{AB}), \quad (4.9)$$

$$\text{gcd}(k, L_{AB}, L_{BC}) = \text{gcd}(k, 0, L_{AB}, L_{BC}) \rightarrow \text{gcd}(k, L_{CA}, L_{AB}, L_{BC}) \quad (4.10)$$

in (4.8), and we eventually obtain

$$\text{Tr}(\rho_{BC}^\Gamma)^{2p} = \frac{1}{k^{2p-1}} \text{gcd}(k, L_{CA}, L_{AB}, L_{BC})^{2p-2} \text{gcd}(k, L_{CA}, L_{AB}). \quad (4.11)$$

Therefore, the logarithmic negativity for the 3-link state (3.5) is given by<sup>19</sup>

$$E_N(B; C) = \lim_{p \rightarrow 1/2} \log \text{Tr}(\rho_{BC}^\Gamma)^{2p} = \log \frac{\text{gcd}(k, L_{CA}, L_{AB})}{\text{gcd}(k, L_{CA}, L_{AB}, L_{BC})}. \quad (4.12)$$

One can see that it reduces to the entanglement entropy between  $B$  and  $C$  when  $L_{CA} = L_{AB} = 0$ . We note again that the expressions (4.11) and (4.12) are conjectures, motivated by the rigorous results (4.7) and (4.8), and further supported by extensive numerical tests.<sup>20</sup>

<sup>19</sup>See the left panel of Fig. 9 for the Venn diagram corresponding to the logarithmic negativity (4.12).

<sup>20</sup>We have numerically verified (4.12) for all three-component links with  $k \leq 18$ , and also tested (4.11) with  $p = 2$  for the same range of  $k$ .

### 4.1 Third-order negativity for three-links

For future reference, we also compute the third-order negativity for three-component links. It is given by<sup>21</sup>

$$\mathcal{E}_3(B;C) := -\frac{1}{2} \log \text{Tr}(\rho_{BC}^\Gamma)^3 = \log \frac{k}{\text{gcd}(k, L_{CA}, L_{AB}, L_{BC})} . \quad (4.13)$$

See appendix D for a non-rigorous proof of this formula. We have also numerically verified (4.13) for all three-component links with  $k \leq 18$ .

## 5 Entanglement structure of links

The link states in Abelian Chern-Simons theory, given by (3.27), are stabilizer states in the context of quantum information theory [21]. In this section, we employ the decomposition properties (5.1) and (5.12) of stabilizer states to explore the physical meanings of  $\text{GM}_1^{(3)}$  and  $E_N$  within this class of states. From these decomposition properties, we derive two relations connecting entanglement entropy, third-order negativity, genuine tri-entropy, and logarithmic negativity (5.18). Using these relations, we verify the consistency of our results (3.25), (4.12), and (4.13). Finally, we propose possible upper and lower bounds for the genuine tri-entropy in general finite-dimensional systems in Section 5.3.

### 5.1 Prime-power qudit stabilizer states

In this section we consider  $N$ -qudit stabilizer states where each qudit has dimension  $k = p^\epsilon$  ( $\epsilon$  is positive integer). We refer to such qudits as power-prime qudits. Any tripartite power-prime qudit stabilizer state  $|\mathbf{S}\rangle_{ABC}$  is locally equivalent to a tensor product of tripartite GHZ <sub>$p$</sub> -states  $|\text{GHZ}_p\rangle_{ABC} \propto \sum_{i=0}^{p-1} |iii\rangle$ , bipartite maximally entangled EPR <sub>$p$</sub> -pairs  $|\text{EPR}_p\rangle_{AB} \propto \sum_{i=0}^{p-1} |ii\rangle$ , and unentangled single qudit states  $|+\rangle$ , that is, there exists a local unitary  $U = U_A \otimes U_B \otimes U_C$  such that [38]<sup>22</sup>

$$\begin{aligned} U_A \otimes U_B \otimes U_C |\mathbf{S}_{p^\epsilon}\rangle_{ABC} &= |\text{GHZ}_p\rangle_{ABC}^{\otimes m_{ABC}} \\ &\otimes |\text{EPR}_p\rangle_{AB}^{\otimes m_{AB}} \otimes |\text{EPR}_p\rangle_{BC}^{\otimes m_{BC}} \otimes |\text{EPR}_p\rangle_{CA}^{\otimes m_{CA}} \\ &\otimes |+\rangle_A^{\otimes m_A} \otimes |+\rangle_B^{\otimes m_B} \otimes |+\rangle_C^{\otimes m_C} , \end{aligned} \quad (5.1)$$

where  $m_{ABC}, m_{AB}, \dots, m_A, \dots$  are non-negative integers. For the product state in (5.1), we have

$$\begin{aligned} \text{GM}_n^{(3)}[\mathbf{S}_{ABC}] &= m_{ABC} \text{GM}_n^{(3)}[\text{GHZ}_{ABC}] \\ &+ m_{AB} \text{GM}_n^{(3)}[\text{EPR}_{AB}] + m_{BC} \text{GM}_n^{(3)}[\text{EPR}_{BC}] + m_{CA} \text{GM}_n^{(3)}[\text{EPR}_{CA}] \\ &+ m_A \text{GM}_n^{(3)}[+_A] + m_B \text{GM}_n^{(3)}[+_B] + m_C \text{GM}_n^{(3)}[+_C] \\ &= m_{ABC} \times \left( \frac{1}{n} - \frac{1}{2} \right) \log p , \end{aligned} \quad (5.2)$$

<sup>21</sup>There is no contradiction between (4.13) and (4.11), since the latter is valid only for integer  $p$ . We also note that our definition of the third-order negativity in (4.13) includes an additional factor of 1/2.

<sup>22</sup>See [39, 40] for previous study on qubit and squarefree qudit case.

where we have used the property that the genuine Rényi multi-entropy vanishes for product states of the form (2.10). Therefore, for stabilizer states, the genuine tri-entropy precisely extracts the number of GHZ<sub>*p*</sub>-states.

Similarly, we consider the logarithmic negativity of Eq. (5.1), where on the right-hand side we use  $E_{\mathcal{N}}^{B;C}$  as a shorthand for  $E_{\mathcal{N}}(B;C)$ :

$$\begin{aligned} E_{\mathcal{N}}(B;C)[\mathbf{S}_{ABC}] &= m_{ABC} E_{\mathcal{N}}^{B;C}[\text{GHZ}_{ABC}] \\ &\quad + m_{AB} E_{\mathcal{N}}^{B;C}[\text{EPR}_{AB}] + m_{BC} E_{\mathcal{N}}^{B;C}[\text{EPR}_{BC}] + m_{CA} E_{\mathcal{N}}^{B;C}[\text{EPR}_{CA}] \quad (5.3) \\ &= m_{BC} \log p , \end{aligned}$$

where we have used the following facts,

$$E_{\mathcal{N}}^{B;C}[\text{GHZ}_{ABC}] = E_{\mathcal{N}}^{B;C}[\text{EPR}_{AB}] = E_{\mathcal{N}}^{B;C}[\text{EPR}_{CA}] = 0 , \quad E_{\mathcal{N}}^{B;C}[\text{EPR}_{BC}] = \log p . \quad (5.4)$$

Therefore, the logarithmic negativity captures the number of EPR-pairs in a stabilizer state. We summarize these two results as follows: for power-prime qudit stabilizer states,

$$2\text{GM}_1^{(3)}[\mathbf{S}_{ABC}] = m_{ABC} \log p , \quad (5.5)$$

$$E_{\mathcal{N}}(B;C)[\mathbf{S}_{ABC}] = m_{BC} \log p . \quad (5.6)$$

We can verify these relations using link states. The number of GHZ-states,  $m_{ABC}$ , in a stabilizer state can be determined by the following quantity [3, 25]<sup>23</sup>,

$$m_{ABC} \log p = S(A) + S(B) + S(C) + \log \text{Tr}(\rho_{BC}^{\Gamma})^3 , \quad (5.7)$$

where the last term is the third-order negativity discussed in Section 4.1. For three-component link states, it is given explicitly by Eq. (4.13). Substituting (3.24) and (4.13) into (5.7), we obtain

$$m_{ABC} \log p = \log \frac{k \cdot \text{gcd}(k, L_{CA}, L_{AB}, L_{BC})^2}{\text{gcd}(k, L_{CA}, L_{AB}) \text{gcd}(k, L_{AB}, L_{BC}) \text{gcd}(k, L_{BC}, L_{CA})} , \quad (5.8)$$

which is nothing but twice the genuine tri-entropy of three-link states (3.25). It follows from Eq. (5.8) that  $m_{ABC}$  must be an integer when  $k = p^{\epsilon}$ .

The number of EPR-pairs (eg.  $m_{BC}$ ,  $m_{CA}$  and  $m_{AB}$ ) in (5.1) can be extracted from the mutual information [3],

$$(2m_{BC} + m_{ABC}) \log p = I(B;C) = S(B) + S(C) - S(BC) . \quad (5.9)$$

Using (3.24) and (5.8), we obtain

$$m_{BC} \log p = \log \frac{\text{gcd}(k, L_{CA}, L_{AB})}{\text{gcd}(k, L_{CA}, L_{AB}, L_{BC})} , \quad (5.10)$$

which is exactly the logarithmic negativity between  $B$  and  $C$  (4.12). One can see that the  $m_{BC}$  in (5.10) is an integer if  $k = p^{\epsilon}$ .

<sup>23</sup>The quantity  $\text{Tr}(\rho_{BC}^{\Gamma})^3$  is one of the six algebraically independent local invariants of pure 3-qubit states [41],

$$I_1 = \langle \Psi | \Psi \rangle , \quad I_2 = \text{Tr}(\rho_C)^2 , \quad I_3 = \text{Tr}(\rho_B)^2 , \quad I_4 = \text{Tr}(\rho_A)^2 , \quad I_5 = \text{Tr}(\rho_{BC}^{\Gamma})^3 , \quad I_6 = \tau_{ABC} ,$$

where  $\tau_{ABC}$  is the 3-tangle [42]. We thank Chen-Te Ma for discussions.

## 5.2 General qudit stabilizer states

Now we turn to more general  $N$ -qudit tripartite stabilizer states  $|\mathbf{S}\rangle_{ABC}$ , where the dimension  $k$  of each qudit is not necessarily a prime-power number. Every integer  $k$  admits a prime factorization,

$$k = p_1^{\epsilon_1} p_2^{\epsilon_2} \cdots p_\ell^{\epsilon_\ell} . \quad (5.11)$$

There always exists some single-qudit unitary transformations  $U_i$  such that [40]

$$U_1 \otimes U_2 \otimes \cdots \otimes U_N |\mathbf{S}\rangle_{ABC} = \bigotimes_{i=1}^{\ell} |\mathbf{S}_i\rangle , \quad (5.12)$$

where  $|\mathbf{S}_i\rangle$  is a stabilizer state on  $N$  qudits of dimension  $p_i^{\epsilon_i}$ , which can be further decomposed as in Eq. (5.1). It is then straightforward to see that for general  $k$  given by Eq. (5.11), Eqs. (5.5) and (5.6) generalize to

$$2\text{GM}_1^{(3)}[\mathbf{S}_{ABC}] = \sum_{i=1}^{\ell} m_{ABC,i} \log p_i , \quad (5.13)$$

$$E_N(B;C)[\mathbf{S}_{ABC}] = \sum_{i=1}^{\ell} m_{BC,i} \log p_i , \quad (5.14)$$

where  $m_{ABC,i}$  and  $m_{BC,i}$  denote the numbers of  $|\text{GHZ}_{p_i}\rangle_{ABC}$  and  $|\text{EPR}_{p_i}\rangle_{BC}$  appearing in the decomposition, respectively. We can thus conclude that for general stabilizer states (with arbitrary qudit dimension), the genuine tri-entropy quantifies the tripartite entanglement generated by GHZ-states, while the logarithmic negativity between  $B$  and  $C$  quantifies the bipartite entanglement generated by EPR-pairs between  $B$  and  $C$ .

Here we use  $|\text{GHZ}_6\rangle$  as a simple example to illustrate (5.13). The state  $|\text{GHZ}_6\rangle$  can be decomposed as

$$\begin{aligned} |\text{GHZ}_6\rangle &= \frac{1}{\sqrt{6}} \sum_{i=0}^5 |iii\rangle = \frac{1}{\sqrt{6}} \sum_{i=00,01,02,10,11,12} |iii\rangle \\ &= \frac{1}{\sqrt{6}} (|000000\rangle + |010101\rangle + |020202\rangle + |101010\rangle + |111111\rangle + |121212\rangle) \quad (5.15) \\ &= \frac{1}{\sqrt{2}} (|000\rangle + |111\rangle) \otimes \frac{1}{\sqrt{3}} (|000\rangle + |111\rangle + |222\rangle) \\ &= |\text{GHZ}_2\rangle \otimes |\text{GHZ}_3\rangle , \end{aligned}$$

from which we can read that  $m_{ABC,1} = m_{ABC,2} = 1$  (this is also consistent with  $6 = 2 \times 3$ ). The genuine tri-entropy of the state  $|\text{GHZ}_6\rangle$  is

$$2\text{GM}_1^{(3)}[\text{GHZ}_6] = \log 6 = \log 2 + \log 3 , \quad (5.16)$$

which is consistent with (5.13).

Using the same method, we also find that for stabilizer states, the second genuine Rényi tri-entropy vanishes:

$$\text{GM}_2^{(3)}[\mathbf{S}_{ABC}] = 0 , \quad (5.17)$$

since the second genuine Rényi tri-entropy is zero for GHZ-states. Eq. (5.17) is consistent with our  $N$ -link results in Section 3.2.2.

For general  $N$ -qudit stabilizer states with arbitrary qudit dimension, although we cannot isolate a specific  $m_{ABC,i}$  using  $\text{GM}_1^{(3)}$ , the following two relations hold:<sup>24</sup>

$$\begin{aligned} S(A) + S(B) + S(C) + \log \text{Tr}(\rho_{BC}^\Gamma)^3 &= 2 \text{GM}_1^{(3)}(A; B; C) , \\ -\frac{1}{2} \log \text{Tr}(\rho_{BC}^\Gamma)^3 - S(A) &= E_N(B; C) . \end{aligned} \quad (5.18)$$

### 5.3 Possible lower and upper bounds of the genuine tri-entropy

From the decomposition properties (5.1) and (5.12) of stabilizer states, together with the fact (5.13) that the genuine tri-entropy counts the total tripartite entanglement generated by GHZ-states, we can see that for stabilizer states, the genuine tri-entropy is bounded by

$$0 \leq \text{GM}_1^{(3)}(A; B; C) \leq \frac{1}{2} \log \left( \min\{\dim \mathcal{H}_A, \dim \mathcal{H}_B, \dim \mathcal{H}_C\} \right) , \quad (5.19)$$

where  $\dim \mathcal{H}_A$  is the dimension of the Hilbert space associated with the subsystem  $A$ . The bound (5.19) is reminiscent of the bound of entanglement entropy<sup>25</sup>,

$$0 \leq S^{(2)}(A; B) = \text{GM}_1^{(2)}(A; B) \leq \log \left( \min\{\dim \mathcal{H}_A, \dim \mathcal{H}_B\} \right) , \quad (5.20)$$

which holds for general finite systems (instead of just stabilizer states). Therefore, it is tempting to conjecture that the bound (5.19) of  $\text{GM}_1^{(3)}(A; B; C)$  also holds for *general finite systems*. We now check several examples. The bound (5.19) is satisfied by the link  $2_1^2 + 2_1^2$  (and the link  $6_3^3$ ) in  $\text{SU}(2)_k$  Chern-Simons theory (3.45)<sup>26</sup>,

$$0 \leq \text{GM}_1^{(3)}[2_1^2 + 2_1^2, \text{SU}(2)_k] = \text{GM}_1^{(3)}[6_3^3, \text{SU}(2)_k] \leq \frac{1}{2} \log(k+1) . \quad (5.21)$$

For the generalized GHZ-state (2.14),

$$0 \leq \text{GM}_1^{(3)}[\widetilde{\text{GHZ}}_k] = -\frac{1}{2} \sum |\lambda_i|^2 \log |\lambda_i|^2 \leq \frac{1}{2} \log k , \quad (5.22)$$

where the equality holds for the  $\text{GHZ}_k$ -state (2.12). For the state  $\psi^{N_A, N_B, N_C}$  in the (1+1)d Chern-Simons theory, its  $\text{GM}_1^{(3)}$  is given by (F.6) and we have

$$0 \leq \text{GM}_1^{(3)}[\psi_m^{N_A, N_B, N_C}] \leq \frac{1}{2} \log |G| , \quad (5.23)$$

where the upper bound is reached when  $G$  is an abelian group. See appendix F for details.

In [16], the authors conjecture that for the W-state  $|\text{W}\rangle = (|001\rangle + |010\rangle + |100\rangle)/\sqrt{3}$ ,

$$S_1^{(3)}[\text{W}] = c_{\text{W}} \log 3 , \quad \text{GM}_1^{(3)}[\text{W}] = \log \frac{2}{3^{3/2-c_{\text{W}}}} , \quad (5.24)$$

<sup>24</sup>These two relations follow directly from the decomposition properties (5.1) and (5.12) of stabilizer states. We check (5.18) for all four-links  $\mathcal{L}^{2,1,1}$  with  $k \leq 7$  (here by “all four-links  $\mathcal{L}^{2,1,1}$ ” we mean that all independent sets of  $(L_{A_1 B}, L_{A_2 B}, L_{B C}, L_{C A_1}, L_{C A_2}) \in \mathbb{Z}^{\otimes 5}$ ), for all five-links  $\mathcal{L}^{3,1,1}$  with  $k \leq 5$ , for all five-links  $\mathcal{L}^{2,2,1}$  with  $k \leq 4$ , for all six-links  $\mathcal{L}^{4,1,1}$  with  $k \leq 3$ , for all six-links  $\mathcal{L}^{2,2,2}$  with  $k \leq 2$ .

<sup>25</sup>By definition the entanglement entropy is the  $q = 2$  multi-entropy, and according to the construction of genuine multi-entropy (Section 2.2), it is also the  $q = 2$  genuine multi-entropy.

<sup>26</sup>For states living on the toric boundary in  $\text{SU}(2)_k$  Chern-Simons theory, the dimension of the associated Hilbert is  $\dim \mathcal{H}(\mathbb{T}^2; \text{SU}(2)_k) = k+1$ .

where  $c_W$  is a numerical constant greater than 1. The  $n = 2, \dots, 6$  Rényi multi-entropies of W-state are [16]

$$\begin{aligned} S_2^{(3)}[W] &= \log 3, & S_3^{(3)}[W] &\approx 0.93 \log 3, & S_4^{(3)}[W] &\approx 0.88 \log 3, \\ S_5^{(3)}[W] &\approx 0.84 \log 3, & S_6^{(3)}[W] &\approx 0.82 \log 3. \end{aligned} \quad (5.25)$$

If one plots  $n$  along the  $x$ -axis and the prefactor of  $\log 3$  along the  $y$ -axis, the data points exhibit a convex ( $\cup$ -shaped) functional behavior, suggesting  $c_W > 1.07$ . Alternatively, plotting  $1/n^2$  versus the same prefactor gives a concave ( $\cap$ -shaped) trend, implying  $c_W < 1.38$ . In summary,  $c_W$  is likely in the range  $1.07 \lesssim c_W \lesssim 1.38$ . Although it remains uncertain whether the W-state exactly satisfies the bound (5.19), the data in (5.25) strongly suggest that it most likely does.

## 6 Conclusion and discussion

In this work, we have studied the multipartite entanglement structure of link states in three-dimensional Chern-Simons theory. For three-component links, we obtained analytic expressions for their Rényi multi-entropy and Rényi entanglement negativity. For  $N$ -component links, we found that the logarithmic negativity counts the bipartite entanglement generated by EPR-pairs, while the genuine multi-entropy counts tripartite entanglement generated by GHZ-states.

There are several directions for future investigation. First, it would be interesting to generalize the analytic expression of  $S_n^{(3)}$  in Eq. (3.23) to the quadripartite or general  $N$ -component case. Second, one may attempt to prove the bounds in Eq. (5.19) for general finite-dimensional systems. Finally, following the ideas of Refs. [23, 24], it would be worthwhile to explore possible connections between multipartite entanglement and quantum anomalies in topological field theories. We expect that our results will shed light on the structure of multipartite entanglement in topological quantum field theories and its potential connections to holography and quantum gravity.

## Acknowledgments

We would like to thank Jinwei Chu and Chen-Te Ma for useful discussions. This work is supported by NSFC grant 12375063 and also supported by Shanghai Oriental Talents Program. YZ is also supported by NSFC 12247103 through Peng Huanwu Center for Fundamental Theory.

## A Second genuine Rényi tri-entropy of generalized GHZ-states (2.14)

The second Rényi tri-entropy of the generalized GHZ-state (2.14) is [1]<sup>27</sup>

$$S_2^{(3)}[\widetilde{\text{GHZ}}_k^N] = -\frac{1}{2} \log \left( \sum_i |\lambda_i|^8 \right), \quad (\text{A.1})$$

---

<sup>27</sup>We use a slightly different definition of the Rényi multi-entropy in (2.6) compared to [1], thus (A.1) has an extra  $1/2$  factor.

and the second Rényi entropy is

$$S_2[\widetilde{\text{GHZ}}_k^N] = -\log \left( \sum_i |\lambda_i|^4 \right). \quad (\text{A.2})$$

Therefore, we have

$$\text{GM}_2^{(3)}[\widetilde{\text{GHZ}}_k^N] = S_2^{(3)} - \frac{3}{2}S_2 = \frac{1}{2} \log \frac{(\sum_i |\lambda_i|^4)^3}{\sum_i |\lambda_i|^8} = \frac{1}{2} \log \frac{(\sum_i p_i^2)^3}{\sum_i p_i^4}, \quad (\text{A.3})$$

where at the last equal sign we introduce  $p_i = |\lambda_i|^2$  and  $\{p_i\}$  is a normalized probability distribution since we consider normalized state (2.14). In this appendix we will prove that the second genuine Rényi tri-entropy of the generalized GHZ-state (A.3) is nonpositive, i.e.,

$$\left( \sum_i p_i^2 \right)^3 \leq \sum_i p_i^4. \quad (\text{A.4})$$

For convenience, we introduce the following notation

$$P_m := \sum_i p_i^m. \quad (\text{A.5})$$

Proof of (A.4).

Step 1: Prove  $(P_2)^2 \leq P_3$ . Consider a discrete random variable  $X$  which takes values  $p_i$  with probabilities  $p_i$ . According to the non-negativity of variance, we have

$$\text{Var}(X) = \mathbb{E}[X^2] - \mathbb{E}[X]^2 = \left( \sum_i p_i^2 \cdot p_i \right) - \left( \sum_i p_i \cdot p_i \right)^2 = P_3 - (P_2)^2 \geq 0. \quad (\text{A.6})$$

Step 2: Prove  $(P_3)^2 \leq P_2 P_4$ . This follows directly from the Cauchy-Schwarz inequality

$$\left( \sum_i u_i v_i \right)^2 \leq \left( \sum_i u_i^2 \right) \left( \sum_i v_i^2 \right) \quad (\text{A.7})$$

by taking  $u_i = p_i^2$  and  $v_i = p_i$ .

From Step 1 and 2, we obtain

$$(P_2)^4 \leq (P_3)^2 \leq P_2 P_4, \quad (\text{A.8})$$

and since  $P_2 > 0$ , we end up with  $(P_2)^3 \leq P_4$ , which is exactly (A.4).

## B Derivation of (3.19)

We take  $n = 3$  as an example. When  $L_{BC} = 0$ , the partition function on the replica space is a summation over  $\beta_{1,\dots,n^2=9}, \chi_{1,\dots,n^2=9}$  of  $1/k^{2n^2} = 1/k^{18}$  with the following  $n^2 = 9$  constraints

$$\begin{aligned} 1 = & \eta[\beta_{14}L_{AB} + \chi_{12}L_{CA}] \eta[\beta_{25}L_{AB} + \chi_{23}L_{CA}] \eta[\beta_{36}L_{AB} + \chi_{31}L_{CA}] \\ & \times \eta[\beta_{47}L_{AB} + \chi_{45}L_{CA}] \eta[\beta_{58}L_{AB} + \chi_{56}L_{CA}] \eta[\beta_{69}L_{AB} + \chi_{64}L_{CA}] \\ & \times \eta[\beta_{71}L_{AB} + \chi_{78}L_{CA}] \eta[\beta_{82}L_{AB} + \chi_{89}L_{CA}] \eta[\beta_{93}L_{AB} + \chi_{97}L_{CA}], \end{aligned} \quad (\text{B.1})$$

with the notation

$$\beta_{ij} := (\beta_i - \beta_j) \bmod k, \quad \chi_{ij} := (\chi_i - \chi_j) \bmod k. \quad (\text{B.2})$$

Using the property (3.8) to the first row in (B.1), we obtain

$$\begin{aligned} & \eta[\beta_{14}L_{AB} + \chi_{12}L_{CA}] \eta[\beta_{25}L_{AB} + \chi_{23}L_{CA}] \eta[\beta_{36}L_{AB} + \chi_{31}L_{CA}] \\ &= \eta[\beta_{14}L_{AB} + \chi_{12}L_{CA}] \eta[\beta_{25}L_{AB} + \chi_{23}L_{CA}] \eta[(\beta_{14} + \beta_{25} + \beta_{36})L_{AB}]. \end{aligned} \quad (\text{B.3})$$

Similarly, applying the property to every row and every column, we get

$$\begin{aligned} 1 = & \eta[\beta_{14}L_{AB} + \chi_{12}L_{CA}] \eta[\beta_{25}L_{AB} + \chi_{23}L_{CA}] \eta[(\beta_{14} + \beta_{25} + \beta_{36})L_{AB}] \\ & \times \eta[\beta_{47}L_{AB} + \chi_{45}L_{CA}] \eta[\beta_{58}L_{AB} + \chi_{56}L_{CA}] \eta[(\beta_{47} + \beta_{58} + \beta_{69})L_{AB}] \\ & \times \eta[(\chi_{12} + \chi_{45} + \chi_{78})L_{CA}] \eta[(\chi_{23} + \chi_{56} + \chi_{89})L_{CA}] \eta[0]. \end{aligned} \quad (\text{B.4})$$

Now we can count the number of solutions. There are

- $k \cdot \gcd(k, L_{CA}, L_{AB})$  possible  $\{\beta_{14}, \chi_{12}\} \in \mathbb{Z}_k^{\otimes 2}$  satisfying  $1 = \eta[\beta_{14}L_{AB} + \chi_{12}L_{CA}]$ . Similar for  $\{\beta_{25}, \chi_{23}\}$ ,  $\{\beta_{47}, \chi_{45}\}$ , and  $\{\beta_{58}, \chi_{56}\}$ .
- $\gcd(k, L_{AB})$  possible  $\beta_{36} \in \mathbb{Z}_k$  satisfying  $1 = \eta[(\beta_{14} + \beta_{25} + \beta_{36})L_{AB}]$  (given  $\beta_{14}$  and  $\beta_{25}$ ). Similar for  $\beta_{69}$ .
- $\gcd(k, L_{CA})$  possible  $\chi_{78} \in \mathbb{Z}_k$  satisfying  $1 = \eta[(\chi_{12} + \chi_{45} + \chi_{78})L_{CA}]$  (given  $\chi_{12}$  and  $\chi_{45}$ ). Similar for  $\chi_{89}$ .
- Note that there are still  $2n^2 - 2(n-1)^2 - (n-1) - (n-1) = 2n$  free variables, each of them can take  $k$  values.

Therefore,

$$\begin{aligned} \mathcal{Z}_{n^2}^{(3)} &= \frac{1}{k^{2n^2}} (k \cdot \gcd(k, L_{CA}, L_{AB}))^{(n-1)^2} \times \gcd(k, L_{AB})^{n-1} \times \gcd(k, L_{CA})^{n-1} \times k^{2n} \\ &= \frac{k^{1-n^2}}{\gcd(k, L_{CA}, L_{AB})^{-(1-n)^2} \times \gcd(k, L_{AB})^{1-n} \times \gcd(k, L_{CA})^{1-n}}, \end{aligned} \quad (\text{B.5})$$

from which we can get (3.19) using the definition of  $S_n^{(3)}$ .

## C Derivation of (4.8)

We take  $p = 3$  as an example. When  $L_{CA} = 0$ , the partition function on the replica space is a summation over  $\beta_{1,\dots,2p}, \chi_{1,\dots,2p}$  of

$$\begin{aligned} & \frac{1}{k^{4p}} \exp \left[ \frac{2\pi i L_{BC}}{k} \left( (\beta_1 - \beta_3)\chi_2 + (\beta_3 - \beta_5)\chi_4 + (\beta_5 - \beta_1)\chi_6 \right. \right. \\ & \quad \left. \left. + (\beta_2 - \beta_4)\chi_3 + (\beta_4 - \beta_6)\chi_5 + (\beta_6 - \beta_2)\chi_1 \right) \right] \end{aligned} \quad (\text{C.1})$$

with the following  $2p = 6$  constraints

$$1 = \eta[(\beta_1 - \beta_2)L_{AB}] \eta[(\beta_2 - \beta_3)L_{AB}] \eta[(\beta_3 - \beta_4)L_{AB}] \times \eta[(\beta_4 - \beta_5)L_{AB}] \eta[(\beta_5 - \beta_6)L_{AB}] \eta[(\beta_6 - \beta_1)L_{AB}] , \quad (\text{C.2})$$

The summation of (C.1) over  $\chi_{1,\dots,2p}$  gives  $2p$  more constraints

$$1 = \eta[(\beta_1 - \beta_3)L_{BC}] \eta[(\beta_3 - \beta_5)L_{BC}] \eta[(\beta_5 - \beta_1)L_{BC}] \times \eta[(\beta_2 - \beta_4)L_{BC}] \eta[(\beta_4 - \beta_6)L_{BC}] \eta[(\beta_6 - \beta_2)L_{BC}] . \quad (\text{C.3})$$

Putting (C.3) and (C.2) together and using the property (3.8) repeatedly, we end up with

$$1 = \eta[(\beta_1 - \beta_2)L_{AB}] \eta[\beta_{13}L_{AB}] \eta[\beta_{35}L_{AB}] \eta[\beta_{24}L_{AB}] \eta[\beta_{46}L_{AB}] \times \eta[\beta_{13}L_{BC}] \eta[\beta_{35}L_{BC}] \eta[\beta_{24}L_{BC}] \eta[\beta_{46}L_{BC}] . \quad (\text{C.4})$$

Now we can count the number of solutions. There are

- $\gcd(k, L_{AB}, L_{BC})$  possible  $\beta_{13} \in \mathbb{Z}_k$  satisfying  $1 = \eta[\beta_{13}L_{AB}] \eta[\beta_{13}L_{BC}]$ . Similar for  $\beta_{35}$ ,  $\beta_{24}$  and  $\beta_{46}$ .
- $k \cdot \gcd(k, L_{AB})$  possible  $\{\beta_1, \beta_2\} \in \mathbb{Z}_k^{\otimes 2}$  satisfying  $1 = \eta[(\beta_1 - \beta_2)L_{AB}]$ .

Therefore, we end up with (4.8)

$$\text{Tr}(\rho_{BC}^\Gamma)^{2p} \Big|_{L_{CA}=0} = \frac{k^{2p}}{k^{4p}} \gcd(k, L_{AB}, L_{BC})^{2p-2} \times k \gcd(k, L_{AB}) , \quad (\text{C.5})$$

where the factor  $k^{2p}$  comes from the summation of  $\chi_{1,\dots,2p}$ .

## D Non-rigorous proof of (4.13)

In this appendix we calculate the quantity  $\text{Tr}(\rho_{BC}^\Gamma)^3$  for the three-link state (3.5). First note that this quantity is permutation symmetric with respect to  $A$ ,  $B$ , and  $C$ , since

$$\text{Tr}(\rho_{BC}^\Gamma)^3 = \langle \mathcal{L}^3 |^{\otimes 3} \sigma_A \sigma_B \sigma_C | \mathcal{L}^3 \rangle^{\otimes 3} \quad (\text{D.1})$$

with  $\sigma_{A,B,C}$  the elements of the permutation group

$$\sigma_A = (1)(2)(3) , \quad \sigma_B = (123) , \quad \sigma_C = (321) . \quad (\text{D.2})$$

The quantity (D.1) is invariant under renaming of the copies. Multiplying  $\sigma_{A,B,C}$  by (321), we obtain

$$(321)\sigma_A = (321) = \sigma_C , \quad (321)\sigma_B = (1)(2)(3) = \sigma_A , \quad (321)\sigma_C = (123) = \sigma_B . \quad (\text{D.3})$$

thus we can see that (D.1) is symmetric about  $A$ ,  $B$ , and  $C$ .

Using (4.6), we obtain

$$\begin{aligned} \text{Tr}(\rho_{BC}^\Gamma)^3 &= \sum_{\beta_{1,2,3}, \chi_{1,2,3}} \frac{1}{k^6} \exp \left[ \frac{2\pi i L_{BC}}{k} (\beta_1(\chi_2 - \chi_3) + \beta_2(\chi_3 - \chi_1) + \beta_3(\chi_1 - \chi_2)) \right] \\ &\quad \times \eta[\beta_{12}L_{AB} - \chi_{12}L_{CA}] \eta[\beta_{23}L_{AB} - \chi_{23}L_{CA}] \eta[\beta_{31}L_{AB} - \chi_{31}L_{CA}] , \end{aligned} \quad (\text{D.4})$$

where we use the notation (B.2). When  $L_{BC} = 0$ , we have

$$\begin{aligned} \text{Tr}(\rho_{BC}^\Gamma)^3|_{L_{BC}=0} &= \sum_{\beta_{1,2,3}, \chi_{1,2,3}} \frac{1}{k^6} \eta[\beta_{12} L_{AB} - \chi_{12} L_{CA}] \eta[\beta_{23} L_{AB} - \chi_{23} L_{CA}] \\ &= k^{-6} \times k^2 \times k \gcd(k, L_{CA}, L_{AB}) \times k \gcd(k, L_{CA}, L_{AB}) \\ &= k^{-2} \gcd(k, L_{CA}, L_{AB})^2, \end{aligned} \quad (\text{D.5})$$

where in the first line we use the property (3.8) to remove one non-independent constraint. Since  $\text{Tr}(\rho_{BC}^\Gamma)^3$  is symmetric about  $A, B, C$ , we should perform the following improvement

$$\gcd(k, L_{CA}, L_{AB}) = \gcd(k, L_{CA}, L_{AB}, 0) \rightarrow \gcd(k, L_{CA}, L_{AB}, L_{BC}), \quad (\text{D.6})$$

thus we end up with (4.13). We also note here that although we do not have a rigorous derivation of (4.13), it passes lots of numerical test (we test it numerically for all 3-links with  $k \leq 18$ ).

## E The Venn diagram

An integer can be uniquely understood as the *multiset*<sup>28</sup> of its prime factors. For example, the multiset corresponding to 180 is  $[2, 2, 3, 3, 5]$ .<sup>29</sup> In this appendix we use the *Venn diagram*<sup>30</sup> to illustrate the relationships between integers.<sup>31</sup> We also present the Venn diagrams of various entanglement measures studied in this paper.

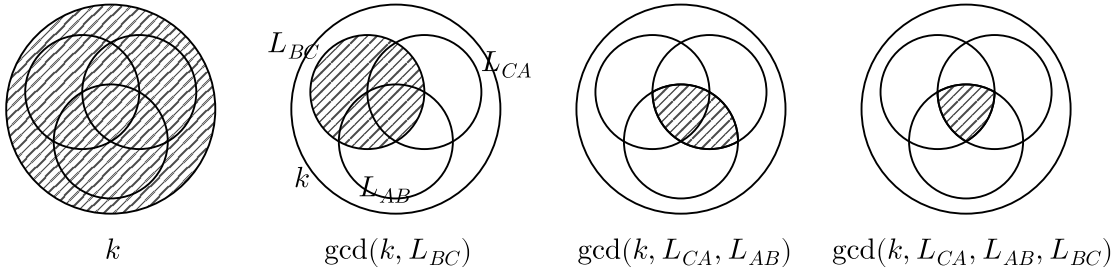


**Figure 8:** From left to right: The Venn diagram of  $k$ ,  $\gcd(k, L_{BC})$ ,  $\gcd(k, L_{CA}, L_{AB})$ ,  $\gcd(k, L_{CA}, L_{AB}, L_{BC})$  respectively.

As shown in Fig. 8, every region represents the multiset corresponding to a nonnegative integer. In this graphical representation, the direct sum of regions corresponds to the multiplication of integers, the direct subtraction of regions corresponds to the division, the intersection of regions corresponds to the gcd function, and the union of regions corresponds to the lcm (least common multiple) function.

<sup>28</sup>A multiset generalizes the notion of a set by permitting elements to occur multiple times [43].

<sup>29</sup>We use the notation  $[\dots]$  to denote a multiset.

<sup>30</sup>The Venn diagram is a diagram style that shows the logical relation between sets [44].

<sup>31</sup>We thank Jinwei Chu for discussions.

The Venn diagrams are very useful in proving inequalities. For example, for the argument of the logarithmic term in  $2\text{GM}_1^{(3)}$  (3.25):

$$\frac{k \cdot \gcd(k, L_{CA}, L_{AB}, L_{BC})^2}{\gcd(k, L_{CA}, L_{AB}) \gcd(k, L_{AB}, L_{BC}) \gcd(k, L_{BC}, L_{CA})}, \quad (\text{E.1})$$

its Venn diagram is shown in the middle part of Fig. 9, from which we can directly see that the inequality (3.26) holds.

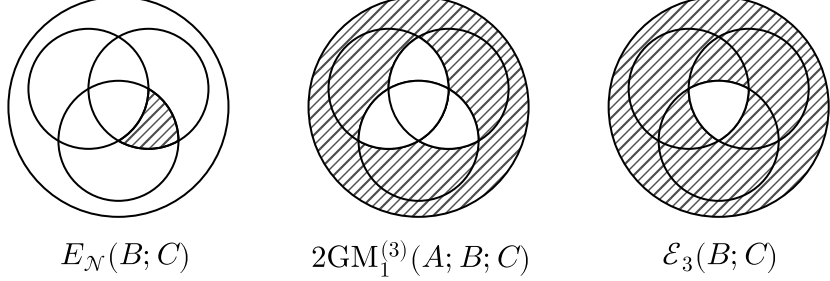


**Figure 9:** From left to right: The Venn diagram of the argument of the log term in the logarithmic negativity (4.12), the genuine multi-entropy (3.25), and the third-order negativity (4.13).

## F Genuine tri-entropy in (1+1)d Chern-Simons theory

In this section we consider the tri-entropy in (1+1)d Chern-Simons theory with finite gauge group  $G$ . Specifically, we follow the setup in section 3 of [22]. The state  $\psi_m^{N_A, N_B, N_C}$  is defined on the  $N = N_A + N_B + N_C$  numbers of  $\mathbb{S}^1$  boundaries of a two-dimensional genus- $m$  manifold, see Fig. 10 for an illustration of the  $N_A = N_B = N_C, m = 1$  case.

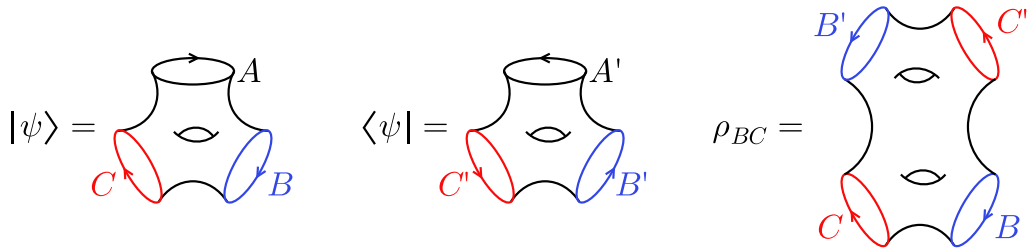


**Figure 10:** The graphical illustration of  $\psi_m^{N_A, N_B, N_C}$  and the unnormalized reduced density matrix  $\rho_{BC}$  with  $N_A = N_B = N_C = 1$  and  $m = 1$ .

Performing the replica trick as in Fig. 2, one can see that the  $n^2$ -replica geometry is a two-manifold with  $g = Nn^2 + 2mn^2 - 2n^2 + 1$  genuses, thus we have

$$\mathcal{Z}_{n^2}^{(3)} = \mathcal{Z}[\Sigma_{Nn^2+2mn^2-2n^2+1}], \quad (\text{F.1})$$

and

$$S_n^{(3)}(A; B; C) = \frac{1}{1-n} \frac{1}{n} \log \frac{\mathcal{Z}[\Sigma_{Nn^2+2mn^2-2n^2+1}]}{\mathcal{Z}[\Sigma_{N+2m-1}]^{n^2}}. \quad (\text{F.2})$$

The partition function (F.1) can be expressed in terms of the group-theoretic properties of the finite gauge group  $G$  as [45]

$$\mathcal{Z}[\Sigma_g] = |G|^{2g-2} \sum_i (\dim R_i)^{2-2g} , \quad (\text{F.3})$$

with  $R_i$  the irreducible representations of the group  $G$  and  $\dim R_i$  their dimensions. Therefore, we can obtain

$$S_1^{(3)}(A; B; C) = -2 \sum_i p_i \log p_i , \quad \text{with } p_i = \frac{(\dim R_i)^{4-4m-2N}}{\sum_j (\dim R_j)^{4-4m-2N}} . \quad (\text{F.4})$$

The entanglement entropy in this setup is [22]

$$S(A; BC) = S(B; CA) = S(C; AB) = - \sum_i p_i \log p_i , \quad (\text{F.5})$$

thus we end up with

$$\text{GM}_1^{(3)}[\psi_m^{N_A, N_B, N_C}] = -\frac{1}{2} \sum_i p_i \log p_i . \quad (\text{F.6})$$

We also note that in this setup the logarithmic negativities (4.1) between  $A$  and  $B$ ,  $B$  and  $C$ ,  $C$  and  $A$  vanish [22],

$$E_N(A; B) = E_N(B; C) = E_N(C; A) = 0 . \quad (\text{F.7})$$

## G Consistency between (3.23) and (G.1)

A recent paper [27] shows that the tripartite multi-entropy for a general tripartite stabilizer state is

$$S^{(3)}(A; B; C) = \frac{1}{2} \log \frac{|G|}{|G_A||G_B||G_C|} + \frac{1}{2} \log \frac{|G|}{|G_{AB} \cdot G_{BC} \cdot G_{CA}|} , \quad (\text{G.1})$$

where  $G$  denotes the stabilizer group, and  $G_A$ ,  $G_B$ ,  $G_C$  are the subgroups that act trivially outside  $A$ ,  $B$ ,  $C$  respectively. Similarly, subgroups  $G_{AB}$ ,  $G_{BC}$ , and  $G_{AC}$  act trivially on  $C$ ,  $A$ , and  $B$  respectively. The subgroup  $G_{AB} \cdot G_{BC} \cdot G_{CA}$  is defined as

$$G_{AB} \cdot G_{BC} \cdot G_{CA} = \{g_1 \cdot g_2 \cdot g_3 \mid g_1 \in G_{AB}, g_2 \in G_{BC}, g_3 \in G_{CA}\} . \quad (\text{G.2})$$

In this appendix, we analytically show that (G.1) is consistent with (3.23).

The stabilizer group of the 3-link state (3.5) is generated by [21]

$$K_A = X_A Z_B^{L_{AB}} Z_C^{L_{CA}} , \quad (\text{G.3})$$

$$K_B = X_B Z_C^{L_{BC}} Z_A^{L_{AB}} , \quad (\text{G.4})$$

$$K_C = X_C Z_A^{L_{CA}} Z_B^{L_{BC}} , \quad (\text{G.5})$$

where  $X_A$  is the generalized Pauli  $X$  operator acting on subregion  $A$ , and the generalized Pauli  $X$  and  $Z$  operators are defined as

$$X = \sum_{h \in \mathbb{Z}_k} |h+1 \pmod{k}\rangle \langle h| , \quad Z = \sum_{h \in \mathbb{Z}_k} \omega^h |h\rangle \langle h| , \quad \omega = e^{2\pi i/k} . \quad (\text{G.6})$$

The stabilizer group  $G$  contains elements of the form  $K_A^m K_B^n K_C^p$  with  $(m, n, p) \in \mathbb{Z}_k^{\otimes 3}$ , thus  $|G| = k^3$ . The subgroup  $G_{BC}$  contains elements of the form  $K_B^p K_C^q$  with

$$pL_{AB} + qL_{CA} \equiv 0 \pmod{k}, \quad (p, q) \in \mathbb{Z}_k^{\otimes 2}, \quad (\text{G.7})$$

which has  $k \gcd(k, L_{CA}, L_{AB})$  sets of  $(p, q)$  solutions. Similarly we have

$$|G_{AB}| = k \gcd(k, L_{BC}, L_{CA}), \quad |G_{BC}| = k \gcd(k, L_{CA}, L_{AB}), \quad |G_{CA}| = k \gcd(k, L_{AB}, L_{BC}). \quad (\text{G.8})$$

The subgroup  $G_A$  contains elements of the form  $K_A^m$  with  $m \in \mathbb{Z}_k$  satisfying  $mL_{AB} \equiv 0 \pmod{k}$  and  $mL_{CA} \equiv 0 \pmod{k}$ , thus  $G_A$  contains  $\gcd(k, L_{CA}, L_{AB})$  number of elements. Therefore we have

$$|G_A| = \gcd(k, L_{CA}, L_{AB}), \quad |G_B| = \gcd(k, L_{AB}, L_{BC}), \quad |G_C| = \gcd(k, L_{BC}, L_{CA}). \quad (\text{G.9})$$

Now let us finally move to the calculation of  $|G_{AB} \cdot G_{BC} \cdot G_{CA}|$ . The subgroup  $\textcolor{red}{G}_{AB} \cdot G_{BC} \cdot \textcolor{blue}{G}_{CA}$  contains elements of the form

$$\begin{aligned} & K_A^m K_B^n \cdot K_B^p K_C^q \cdot \textcolor{blue}{K}_C^r K_A^s \\ &= X_A^{m+s} X_B^{p+n} X_C^{r+q} Z_A^{(r+q)L_{CA} + (p+n)L_{AB}} Z_B^{(m+s)L_{AB} + (r+q)L_{BC}} Z_C^{(p+n)L_{BC} + (m+s)L_{CA}}, \end{aligned} \quad (\text{G.10})$$

with  $(m, n, p, q, r, s) \in \mathbb{Z}_k^{\otimes 6}$  and satisfying

$$\begin{cases} mL_{CA} + nL_{BC} \equiv 0 \pmod{k}, \\ pL_{AB} + qL_{CA} \equiv 0 \pmod{k}, \\ rL_{BC} + sL_{AB} \equiv 0 \pmod{k}. \end{cases} \quad (\text{G.11})$$

Now we need to figure out how many *different* elements are there. We already know  $|G_{AB}|$ ,  $|G_{BC}|$  and  $|G_{CA}|$ . However, when

$$\begin{cases} m+s \equiv 0 \pmod{k}, \\ p+n \equiv 0 \pmod{k}, \\ r+q \equiv 0 \pmod{k}, \end{cases} \quad (\text{G.12})$$

Eq. (G.10) becomes identity, thus we need to divide by the degeneracy,

$$|G_{AB} \cdot G_{BC} \cdot G_{CA}| = \frac{|G_{AB}| \cdot |G_{BC}| \cdot |G_{CA}|}{\# \text{ of solutions of (G.14)}}, \quad (\text{G.13})$$

with (G.14) the combination of (G.11) and (G.12),

$$\begin{cases} mL_{CA} - pL_{BC} \equiv 0 \pmod{k}, \\ pL_{AB} - rL_{CA} \equiv 0 \pmod{k}, \\ rL_{BC} - mL_{AB} \equiv 0 \pmod{k}, \end{cases} \iff \begin{pmatrix} B & -A & \\ C & -B & \\ -C & A & \end{pmatrix} \begin{pmatrix} m \\ p \\ r \end{pmatrix} \equiv \mathbf{0} \pmod{k}, \quad (\text{G.14})$$

where we introduce  $A := L_{BC}$ ,  $B := L_{CA}$  and  $C := L_{AB}$ .

The number of solutions of a system of congruences

$$M\mathbf{x} \equiv \mathbf{0} \pmod{k}, \quad \mathbf{x} \in \mathbb{Z}_k^n \quad (\text{G.15})$$

can be determined using the Smith normal form (SNF) [46] of the corresponding coefficient matrix  $M$ . The main idea is to find two nonsingular matrices  $U$  and  $V$  such that

$$UMV = D = \text{diag}(d_1, d_2, d_3, \dots, d_r, 0, \dots, 0), \quad (\text{G.16})$$

where the diagonal elements  $d_i$  satisfy  $d_i|d_{i+1}$ , and  $r = \text{rank}(M)$ . Using this method, one can transform the original system of congruences to

$$D\mathbf{y} \equiv \mathbf{0} \pmod{k}, \quad \mathbf{y} \in \mathbb{Z}_k^n, \quad (\text{G.17})$$

with  $\mathbf{y} = V^{-1}\mathbf{x}$ . The diagonal element  $d_i$  can be computed as

$$d_i = \frac{m_i(M)}{m_{i-1}(M)}, \quad (\text{G.18})$$

where  $m_i(M)$  equals the greatest common divisor of the determinants of all  $i \times i$  minors of the matrix  $M$  and  $m_0(M) = 1$ . Then the number of solutions is

$$k^{(n-r)} \prod_{i=1}^r \gcd(k, d_i). \quad (\text{G.19})$$

In our case,  $n = 3$ ,  $r = 2$ , and it can be easily computed that

$$\begin{cases} m_1 = \gcd(A, B, C), \\ m_2 = \gcd(A^2, B^2, C^2, AB, BC, CA). \end{cases} \quad (\text{G.20})$$

The  $m_2$  in (G.20) can be further simplified as

$$\begin{aligned} m_2 &= \gcd(A^2, B^2, C^2, AB, BC, CA) \\ &= \gcd(A, B, C)^2 \gcd(a^2, b^2, c^2, ab, bc, ca) \\ &= \gcd(A, B, C)^2 \gcd(\gcd(a^2, ab, ac), \gcd(ba, b^2, bc), \gcd(ca, cb, c^2)) \\ &= \gcd(A, B, C)^2 \gcd(a \gcd(a, b, c), b \gcd(a, b, c), c \gcd(a, b, c)) \\ &= \gcd(A, B, C)^2, \end{aligned} \quad (\text{G.21})$$

where in the second line we introduce

$$a = \frac{A}{\gcd(A, B, C)}, \quad b = \frac{B}{\gcd(A, B, C)}, \quad c = \frac{C}{\gcd(A, B, C)}, \quad (\text{G.22})$$

and thus we have  $\gcd(a, b, c) = 1$ , which is applied to the fourth line of (G.21).

With the results of  $m_1$  and  $m_2$ , according to (G.18) and (G.19) we have

$$\# \text{ of solutions of (G.14)} = k \gcd(k, \gcd(L_{BC}, L_{CA}, L_{AB}))^2, \quad (\text{G.23})$$

and thus

$$|G_{AB} \cdot G_{BC} \cdot G_{CA}| = \frac{k \gcd(k, L_{BC}, L_{CA}) \cdot k \gcd(k, L_{CA}, L_{AB}) \cdot k \gcd(k, L_{AB}, L_{BC})}{k \gcd(k, L_{BC}, L_{CA}, L_{AB})^2}. \quad (\text{G.24})$$

Inserting  $|G| = k^3$ , (G.9) and (G.24) into (G.1), we obtain explicitly (3.23) with  $n = 1$ .

## References

- [1] A. Gadde, V. Krishna and T. Sharma, *New multipartite entanglement measure and its holographic dual*, *Phys. Rev. D* **106** (2022) 126001 [[2206.09723](#)].
- [2] M. Walter, D. Gross and J. Eisert, *Multi-partite entanglement*, [1612.02437](#).
- [3] S. Nezami and M. Walter, *Multipartite Entanglement in Stabilizer Tensor Networks*, *Phys. Rev. Lett.* **125** (2020) 241602 [[1608.02595](#)].
- [4] Y. Zou, K. Siva, T. Soejima, R.S.K. Mong and M.P. Zaletel, *Universal tripartite entanglement in one-dimensional many-body systems*, *Phys. Rev. Lett.* **126** (2021) 120501 [[2011.11864](#)].
- [5] G. Penington, M. Walter and F. Witteveen, *Fun with replicas: tripartitions in tensor networks and gravity*, *JHEP* **05** (2023) 008 [[2211.16045](#)].
- [6] A. Gadde, J. Harper and V. Krishna, *Multi-invariants and bulk replica symmetry*, *JHEP* **06** (2025) 116 [[2411.00935](#)].
- [7] A. Gadde, V. Krishna and T. Sharma, *Towards a classification of holographic multi-partite entanglement measures*, *JHEP* **08** (2023) 202 [[2304.06082](#)].
- [8] A. Gadde, S. Jain, V. Krishna, H. Kulkarni and T. Sharma, *Monotonicity conjecture for multi-party entanglement. Part I*, *JHEP* **02** (2024) 025 [[2308.16247](#)].
- [9] A. Gadde, S. Jain and H. Kulkarni, *Multi-partite entanglement monotones*, [2406.17447](#).
- [10] J. Harper, T. Takayanagi and T. Tsuda, *Multi-entropy at low Renyi index in 2d CFTs*, *SciPost Phys.* **16** (2024) 125 [[2401.04236](#)].
- [11] B. Liu, J. Zhang, S. Ohyama, Y. Kusuki and S. Ryu, *Multiwavefunction overlap and multientropy for topological ground states in (2+1) dimensions*, *Phys. Rev. B* **112** (2025) 125160 [[2410.08284](#)].
- [12] Y. Sheffer, A. Stern and E. Berg, *Extracting Topological Spins from Bulk Multipartite Entanglement*, *Phys. Rev. Lett.* **135** (2025) 086601 [[2502.12259](#)].
- [13] M.-K. Yuan, M. Li and Y. Zhou, *Reflected Multientropy and Its Holographic Dual*, *Phys. Rev. Lett.* **135** (2025) 091604 [[2410.08546](#)].
- [14] N. Iizuka, A. Miyata and M. Nishida, *Multipartite Markov Gaps and Entanglement Wedge Multiway Cuts*, [2507.15262](#).
- [15] N. Iizuka, S. Lin and M. Nishida, *Black hole multi-entropy curves — secret entanglement between Hawking particles*, *JHEP* **03** (2025) 037 [[2412.07549](#)].
- [16] N. Iizuka and M. Nishida, *Genuine multientropy and holography*, *Phys. Rev. D* **112** (2025) 026011 [[2502.07995](#)].
- [17] N. Iizuka, S. Lin and M. Nishida, *More on genuine multientropy and holography*, *Phys. Rev. D* **112** (2025) 066014 [[2504.16589](#)].
- [18] J. Harper, A. Mollabashi, T. Takayanagi and K. Tasuki, *Multi-entropy and the Dihedral Measures at Quantum Critical Points*, [2506.10396](#).
- [19] V. Balasubramanian, J.R. Fliss, R.G. Leigh and O. Parrikar, *Multi-Boundary Entanglement in Chern-Simons Theory and Link Invariants*, *JHEP* **04** (2017) 061 [[1611.05460](#)].

[20] S. Dwivedi, V.K. Singh, S. Dhara, P. Ramadevi, Y. Zhou and L.K. Joshi, *Entanglement on linked boundaries in Chern-Simons theory with generic gauge groups*, *JHEP* **02** (2018) 163 [[1711.06474](#)].

[21] V. Balasubramanian, M. DeCross, J. Fliss, A. Kar, R.G. Leigh and O. Parrikar, *Entanglement Entropy and the Colored Jones Polynomial*, *JHEP* **05** (2018) 038 [[1801.01131](#)].

[22] S. Dwivedi, A. Addazi, Y. Zhou and P. Sharma, *Multi-boundary entanglement in Chern-Simons theory with finite gauge groups*, *JHEP* **04** (2020) 158 [[2003.01404](#)].

[23] L.-Y. Hung, Y.-S. Wu and Y. Zhou, *Linking Entanglement and Discrete Anomaly*, *JHEP* **05** (2018) 008 [[1801.04538](#)].

[24] Y. Zhou, *3d One-form Mixed Anomaly and Entanglement Entropy*, *JHEP* **07** (2019) 091 [[1904.06924](#)].

[25] G. Salton, B. Swingle and M. Walter, *Entanglement from Topology in Chern-Simons Theory*, *Phys. Rev. D* **95** (2017) 105007 [[1611.01516](#)].

[26] V. Balasubramanian and C. Cummings, *Multipartite entanglement structure of fibered link states*, *Phys. Rev. D* **111** (2025) 105020 [[2502.19466](#)].

[27] S. Akella, *Tripartite entanglement in the HaPPY code is not holographic*, [2510.08520](#).

[28] H.J. Briegel and R. Raussendorf, *Persistent Entanglement in Arrays of Interacting Particles*, *Phys. Rev. Lett.* **86** (2001) 910 [[quant-ph/0004051](#)].

[29] J.K. Stockton, J.M. Geremia, A.C. Doherty and H. Mabuchi, *Characterizing the entanglement of symmetric many-particle spin-1/2 systems*, *Phys. Rev. A* **67** (2003) 022112 [[quant-ph/0210117](#)].

[30] E. Witten, *Quantum Field Theory and the Jones Polynomial*, *Commun. Math. Phys.* **121** (1989) 351.

[31] M. Hein, W. Dür, J. Eisert, R. Raussendorf, M. Van den Nest and H.J. Briegel, *Entanglement in Graph States and its Applications*, [quant-ph/0602096](#).

[32] M. Hein, J. Eisert and H.J. Briegel, *Multiparty entanglement in graph states*, *Phys. Rev. A* **69** (2004) 062311 [[quant-ph/0307130](#)].

[33] D. Schlingemann, *Cluster states, algorithms and graphs*, [quant-ph/0305170](#).

[34] W. Tang, S. Yu and C. Oh, *Greenberger-horne-zeilinger paradoxes from qudit graph states*, *Phys. Rev. Lett.* **110** (2013) 100403 [[1206.2718](#)].

[35] L. Chen and D. Zhou, *Graph states of prime-power dimension from generalized cnot quantum circuit*, *Scientific Reports* **6** (2016) 27135 [[1507.05386](#)].

[36] A. Peres, *Separability criterion for density matrices*, *Phys. Rev. Lett.* **77** (1996) 1413 [[quant-ph/9604005](#)].

[37] G. Vidal and R.F. Werner, *Computable measure of entanglement*, *Phys. Rev. A* **65** (2002) 032314 [[quant-ph/0102117](#)].

[38] Y. Wong and L. Jiang, *Local unitary decomposition of tripartite arbitrary leveled qudit stabilizer states into p-level-qudit EPR and GHZ state*, [2507.09416](#).

[39] S. Bravyi, D. Fattal and D. Gottesman, *GHZ extraction yield for multipartite stabilizer states*, *Journal of Mathematical Physics* **47** (2006) 062106 [[quant-ph/0504208](#)].

- [40] S.Y. Looi and R.B. Griffiths, *Tripartite Entanglement in Qudit Stabilizer States and Application in Quantum Error Correction*, *Phys. Rev. A* **84** (2011) 052306 [[1107.1761](https://arxiv.org/abs/1107.1761)].
- [41] A. Sudbery, *On local invariants of pure three-qubit states*, *Journal of Physics A Mathematical General* **34** (2001) 643 [[quant-ph/0001116](https://arxiv.org/abs/quant-ph/0001116)].
- [42] V. Coffman, J. Kundu and W.K. Wootters, *Distributed entanglement*, *Phys. Rev. A* **61** (2000) 052306 [[quant-ph/9907047](https://arxiv.org/abs/quant-ph/9907047)].
- [43] Wikipedia contributors, “Multiset — Wikipedia, the free encyclopedia.” <https://en.wikipedia.org/w/index.php?title=Multiset&oldid=1298654476>, 2025.
- [44] Wikipedia contributors, “Venn diagram — Wikipedia, the free encyclopedia.” [https://en.wikipedia.org/w/index.php?title=Venn\\_diagram&oldid=1297058976](https://en.wikipedia.org/w/index.php?title=Venn_diagram&oldid=1297058976), 2025.
- [45] D.S. Freed, *Lectures on topological quantum field theory*, in *Integrable Systems, Quantum Groups, and Quantum Field Theories*, L.A. Ibort and M.A. Rodríguez, eds., (Dordrecht), pp. 95–156, Springer Netherlands (1993), [DOI](https://doi.org/10.1007/978-94-017-2200-8_3).
- [46] Wikipedia contributors, “Smith normal form — Wikipedia, the free encyclopedia.” [https://en.wikipedia.org/w/index.php?title=Smith\\_normal\\_form&oldid=1288152750](https://en.wikipedia.org/w/index.php?title=Smith_normal_form&oldid=1288152750), 2025.